People's Democratic Republic of Algeria

Ministry Of Higher Education and Scientific Research

Mouloud Mammeri University of Tizi-Ouzou

Faculty Of Construction Engineering

Hydraulics Department

MASTER'S THESIS

Submitted in partial fulfilment of the requirements for the

Master's degree in the field of Hydraulics with a specialization in Hydraulic Structures.

Title:

Effect Of Roughness on Velocity Distribution in Open-Channel Flow

by

Thiziri IDDIR

Lilia BOUKHEBOU

Jury:

Mr. KHATTAOUI Mohammed	Professor	Supervisor	UMMTO
Mr. ABSI Rafik	Professor	Co-Supervisor	ECAM-EPMI
Mr. ZAMOUM Said	MCB	President	UMMTO
Mr. HAMANI Sofiane	MAB	Examiner	UMMTO

Academic year 2022/2023

Acknowledgments

We want to start by expressing our deep gratitude to Professor KHATTAOUI Mohammed. Throughout our research, he has been a constant source of guidance and patience. His wealth of experience not only inspired us but also fueled our determination to complete this thesis.

Furthermore, we'd like to extend our sincere thanks to Professor ABSI Rafik for his invaluable support and guidance. His extensive expertise has been instrumental in helping and guiding us along the way, and his unwavering patience has been truly appreciated.

Finally, we want to express our deep appreciation to our families for the motivation and financial assistance they provided. Their support was instrumental in our ability to complete this thesis.

Thiziri IDDIR

Lilia BOUKHEBOU

Mouloud Mammeri University of Tizi-Ouzou

♡ Dedication ♡

I dedicate this thesis to my parents, Said and Samia, and my brother, Jugurtha, in deep appreciation of their unwavering support. Their guidance, influence, and encouragement have been the bedrock of my success.

I also extend my heartfelt gratitude to my family and friends for their unwavering belief in my journey. This work stands as a tribute to the irreplaceable roles they've played in my life.

No language can adequately convey the depth of my love and gratitude for all of you.

In pages filled with knowledge and dreams,
A journey embarked, or so it seems.
With Said and Samia, and Jugurtha by my side,
Through every challenge, you've been my guide.

To family and friends, my heartfelt delight,
Your unwavering faith shines so bright.
This thesis, a tribute to your roles so true,
I dedicate it with love, thanks to each of you.

No words can express the depth of my heart,
For you've played the most special part.
With love and gratitude, my story's told,
In your support, I've found my gold.

♡ Thiziri (Yasmine) ♡

Dédicaces

À mes chers parents, Ouiza et Kamel,

Votre amour inébranlable et votre soutien constant ont été la source de ma force et de ma détermination tout au long de ce voyage académique. Votre foi en moi m'a toujours poussé à donner le meilleur de moi-même.

À mon grand-père bien-aimé, Mokran,

Bien que tu ne sois plus parmi nous, ton héritage de sagesse et de persévérance continue de m'inspirer. Ton souvenir est gravé dans mon cœur à jamais.

À mon frère, Amine, et ma sœur, Thiziri,

Votre présence et votre soutien ont été un véritable réconfort dans les moments difficiles. Vous êtes ma famille, ma force, et ma fierté.

À mes tantes Fazia, Marie, et Kahina, ainsi qu'à mon oncle Mouloud,

Votre soutien moral inestimable a été une lumière dans les moments sombres de mon parcours académique. Votre encouragement a été essentiel.

À mes petits cousins et cousines, les anges : Mohammed Mokran, Syfax, Emily, Léa, Orélia, Cérine,

Votre amour inconditionnel et votre présence joyeuse ont apporté une dimension spéciale à ma vie.

Vous êtes la preuve vivante de l'amour et du bonheur au sein de notre famille.

Et à toute ma famille,

Votre soutien, votre amour, et votre unité ont été la pierre angulaire de ma réussite académique. Cette réalisation est le fruit de notre solidarité et de notre affection.

Je vous dédie ce mémoire avec tout mon amour et ma reconnaissance.

LILIA.M

ملخص

تهدف هذه الدراسة إلى دراسة تأثيرات خشونة السطح على التدفقات المضطربة ذات السطح الحر. وبالتحديد، تركز على سيناريو وجود ظاهرة "الانخفاض"، والتي تحدث عندما تكون السرعة القصوى تحت السطح الحر. بعد استعراض المفاهيم الأساسية والدراسات السابقة، تم إنشاء ملفات تعريف السرعة لطبقات ناعمة وخشنة باستخدام تعبيرات تحليلية من الأدبيات. ثم يتم مقارنة هذه الملفات المحسوبة بالتفصيل مع القياسات التجريبية المستخرجة من مقال رئيسي كتبه تاتشي وآخرون (2004). تكشف التحليل عن توافق وثيق بين توزيعات السرعة المحسوبة والبيانات المقاسة، حتى بالنسبة للطبقات الخشنة. تؤكد النتائج صحة النماذج التحليلية للتنبؤ بالتدفقات على الأسطح الخشنة. تقدم هذه الدراسة أدلة جديدة على أن النماذج التحليلية يمكن أن تعيد إنتاج تأثير خشونة السطح بدقة. تساهم المعرفة المكتسبة في سد الفجوة بين التمثيلات الرياضية والواقع المادي في التدفقات المضطربة على الجدران الخشنة.

كلمات مفتاحية :التدفق ذو السطح الحر، التيار المضطرب، النمذجة، الخشونة، قوانين الجدار

Resumé :

Cette recherche vise à étudier les effets de la rugosité de surface sur les écoulements turbulents à surface libre. Plus précisément, elle se concentre sur le scénario de l'existence du phénomène du "dip," qui se produit lorsque la vitesse maximale se trouve en dessous de la surface libre. Après avoir examiné les concepts fondamentaux et les études précédentes, des profils de vitesse pour des lits lisses et rugueux sont générés à l'aide d'expressions analytiques de la littérature. Ces profils calculés sont ensuite comparés de manière exhaustive aux mesures expérimentales extraites d'un article clé rédigé par Tachie et al. (2004). L'analyse révèle une étroite concordance entre les distributions de vitesse calculées et les données mesurées, même pour les lits rugueux. Les résultats confirment la validité des modèles analytiques pour prédire les écoulements sur des surfaces rugueuses. Cette recherche apporte de nouvelles preuves que les modèles analytiques peuvent reproduire avec précision l'effet de la rugosité de surface. Les connaissances acquises contribuent à combler l'écart entre les représentations mathématiques et la réalité physique dans les écoulements turbulents sur des parois rugueuses.

Mots Clés : Écoulement à surface libre, Turbulence, Modélisation, Rugosité, Lois de paroi

Abstract

This research aims to investigate the impact of surface roughness on turbulent free-surface flows, with a specific focus on the "dip phenomenon" where the maximum velocity is below the free surface. After reviewing fundamental concepts and previous studies, velocity profiles for both smooth and rough beds are generated using analytical expressions from the literature. These computed profiles are then extensively compared to experimental data extracted from a significant study by Tachie et al. (2004). The analysis demonstrates a close agreement between the calculated velocity distributions and measured data, even for rough beds. These findings reaffirm the reliability of analytical models in predicting flows over rough surfaces, contributing new evidence to support this. The knowledge gained from this research helps bridge the gap between mathematical representations and the physical reality of turbulent flows over rough surfaces.

Keywords: Free-surface flow, Turbulence, Modeling, Roughness, Boundary laws.

Table of contents

List of Figures

List of Tables

list of symbols

Ar = open-channel aspect ratio (Ar = b/h)

b = open-channel width

D_h =Hydraulic diameter

F = Froude number (F= U/(gh)^$^{1/2}$)

g = gravitational acceleration

h = free-surface flow depth or the distance from the wall to the axis of symmetry

I_s = free surface slope.

k = Roughness height

k_s^+, h_s^+ = Roughness Reynolds number, ($k_s^+ = k_s u_* / \nu$)

k_s , h_s = Equivalent sand-grain roughness

Re = Reynolds number

Re_* = friction Reynolds number ($Re_* = h u_* / \nu$)

Ua, U+ = dimensionless streamwise mean velocity ($U^+ = U/U_*$)

Ua,max = maximal value of Ua at dip position Ua($\xi = \xi dip$)

w(ξ) =Fonction de cisaillage de Coles

y = vertical distance from bed

y^+ = Dimensionless wall normal-wall direction, ($y^+ = y u_* / \nu$)

y0 = the distance at which the velocity is hypothetically equal to zero.

α = parameter related to Ar and ξdip

δ = channel half-width or boundary layer thikness

ΔU^+ =Roughness function

κ = Kármán constant (≈ 0.41)

ν = kinematic viscosity

νt = eddy viscosity

ξ = dimensionless distance from bed ($\xi = y/h$)

$\xi 0$ = relative roughness (= y0/h)

ξdip = dip distance of maximum velocity

Π = Coles parameter

ρ = density of fluid

τ = shear stress

τ_p = wall shear stress ($\tau_p = \rho\, u_*^2$)

u_* = wall friction velocity

All variables with the superscript of + are those non-dimensionalized by u_* and ν

Abreviations

CFD = Computational fluid dynamics

DNS = Direct numerical simulation

RANS = Reynolds-averaged Navier-Stokes

LES =Large Eddy Simulations

RST= Reynolds-Stress Transport

TKE = Turbulent kinetic energy

sDMLW-law = simple dip-modified-log-wake law

ODE = ordinary differential equation

LDA=Laser Doppler Anemometer

LDV: Laser Doppler Velocimetry

General Introduction

The behaviour of turbulent flows over rough surfaces is a complex phenomenon with significant implications in hydraulic engineering and environmental fluid mechanics. In open channels, the presence of roughness elements on the bed strongly influences the velocity distribution, especially near the wall region. This research focuses specifically on the scenario where the maximum velocity manifests beneath the free surface, known as the dip phenomenon. The aim is to assess the validity of analytical models in representing velocity profiles over rough beds exhibiting this phenomenon.

Understanding the Significance

To fully appreciate the significance of our study, let's consider its real-world relevance. Imagine a river flowing through a diverse landscape, where the riverbed is studded with an assortment of roughness elements, from natural rocks to engineered structures. Understanding how these rough surfaces affect the behaviour of flowing water holds the key to efficiently managing water systems, protecting ecosystems from erosion, and preserving natural habitats. Our research, therefore, unfolds as a vital piece in the puzzle of how the natural world functions.

Our Research Journey

This journey begins with an exploration of fundamental concepts in turbulent flows over both smooth and rough surfaces. Chapters 1 and 2 lay the groundwork, introducing the dynamics of free-surface flows, the intricate world of turbulence, the role of surface roughness, and the evolution of research in this field.

Chapter 3 details the methodology employed in our research. Without conducting physical experiments, we opted for a non-experimental approach, relying on the meticulous analysis of pre-existing data from articles and literature. We emphasize the selection of Mark F. Tachie, Donald J. Bergstrom, and Ram Balachandar's 2004 article, which forms the cornerstone of our research. The use of the "Plot Digitizer" software is explained, and the role of velocity profiles generated through mathematical equations, derived from Rafik Absi's (2011) work, is highlighted.

Chapter 4 represents the heart of our research, where we analyse the data meticulously. We present the velocity profile data from Tachie's study, compare it with computational models, and discuss the findings. This chapter highlights the impact of surface roughness on water flow, the "dip phenomenon," and the practical implications of our research, emphasizing the alignment of computational models with experimental data.

Chapter 1: Fundamental Concepts in Turbulent Free-Surface Flow

1.1 Introduction

This chapter aims to present the main concepts and phenomena associated with turbulent free-surface flows over smooth and rough beds. First, we introduce the concept of free-surface flow and its characteristics. Then, we define turbulence and its effects on flows, particularly within the boundary layer. Next, we discuss surface roughness and its influence on the dynamics of turbulent flows. We present key physical parameters for characterizing roughness, such as the equivalent roughness length. We then describe the different flow regimes over rough beds. Finally, we detail the structure of the turbulent boundary layer over smooth and rough surfaces, as well as the methods for estimating wall parameters like boundary layer thickness or friction velocity. This literature review aims to provide the theoretical foundations for understanding the dynamics of turbulent flows over rough beds, highlighting the key challenges and parameters that will be useful for the rest of the study.

1.2 Basic Concepts of Hydraulic Flows

1.2.1 Free-Surface and Pressurized Flows

In the field of hydraulics, "flow" simply means the movement of water through various hydraulic systems, including channels, rivers, dams, pipes, reservoirs... This flow can be divided into two main categories: free-surface flows and pressurized flows.

Free-surface flows, our first category, happen when the surface of the fluid is in direct contact with the surrounding air, resulting in the pressure at this free surface matching atmospheric pressure. These flows are primarily driven by gravity, as the natural pull of gravity guides the liquid downstream, following the slope or gradient of the surface.

To put it simply, imagine a river flowing through a valley, in this scenario, the river's surface meets the open air, and the pressure at this surface matches the atmospheric pressure. It's a classic example of free surface flow in action.

Pressurized flows occur when the fluid is confined within a closed pipe or channel. This means that the pressure at any point within the fluid is greater than the atmospheric pressure. Pressurized flows are common in plumbing, irrigation, and industrial applications.

1.2.2 Flow Classification

In hydraulics, flows can be classified based on several criteria, including velocity, fluid viscosity, channel or conduit geometry, and the forces acting on the fluid. Here are some of the commonly used methods for classifying flows in hydraulics.

a) Steady vs Unsteady:

Steady Flow: This happens when the flow characteristics like velocity and pressure remain constant over time. It's like a continuous and stable stream.

Unsteady Flow (or Transient Flow): In contrast, unsteady flow occurs when these characteristics vary with time, such as when you quickly turn a faucet on or off.

b) Uniform vs Non-uniform:

Uniform Flow: In uniform flow, the water flows evenly, with a constant velocity across a specific area. Think of it as parallel and regular streams.

Non-uniform Flow: Non-uniform flow is when the velocity varies across the area, creating irregular streams that may curve or converge.

c) Viscous vs. Non-viscous:

Viscous Flow: Viscous flow is influenced by the thickness (viscosity) of the fluid. It's like honey flowing slowly due to its thickness. Viscous forces play a significant role and create resistance.

Non-viscous Flow (or Ideal Flow): Non-viscous flow is where fluid viscosity is negligible. It's similar to pure water flowing smoothly without the influence of viscosity. Viscous forces are minimal in this case.

d) Laminar vs Turbulent:

Laminar Flow: In laminar flow, water molecules move in an orderly manner, following well-defined paths. It's like a calm and organized river. This happens at lower speeds or with thick viscous fluids.

Turbulent Flow: Turbulent flow, on the other hand, is chaotic. Water moves erratically with swirls, eddies, and intense speed changes, resembling a fast and turbulent river. This occurs at high speeds or with thin, less viscous fluids.

With this understanding of turbulent flow in mind, it's essential to define turbulence within the context of fluid dynamics. So, **what exactly is turbulence in the world of fluid dynamics?**

1.3 Understanding Turbulence in Flows

1.3.1 Definition of Turbulence

Turbulence is a complex phenomenon that cannot be easily defined. It is characterized by **its effects**, such as chaotic changes in pressure and flow velocity, and it is a complicated and irregular movement observed in fluid flows, such as gases or liquids, when they flow near solid surfaces or interact with neighboring flows[1].

It happens because the flow becomes unstable and transitions from smooth to chaotic behavior either suddenly or gradually. The defining feature of turbulence is that it has a wide range of different-sized structures. Energy from larger structures gets transferred to smaller ones, keeping the turbulence going. The size of the biggest structures is limited by the shape of the flow, while the smallest ones are restricted by properties like viscosity [1]

Turbulence is not dependent on the type of fluid but on the flow itself, and it is only observed in flows with some viscosity [1]. Turbulence is essential for mixing and dispersing fluids on various scales, from stirring a cup of coffee to large-scale atmospheric phenomena, like storms [2].

1.3.2 Numerical Simulations and Turbulence Models

Numerical methods, like Computational Fluid Dynamics (CFD), rely on computer simulations use the Navier-Stokes equations to describe how fluids behave, to better understand turbulence in fluid flow, engineers use different approaches such as: Direct Numerical Simulation (DNS), which provides the highest accuracy by directly solving the entire range of turbulence without using models.

Large Eddy Simulations (LES), which directly resolve the larger turbulent structures and model the smaller ones. (RANS) which stands for Reynolds-Averaged Navier-Stokes, is a widely used approach due to its ability to provide a balance between acceptable accuracy and reasonable computational cost. The RANS equations are typically paired with a turbulence model, which is a simplified description of the behavior of turbulence in order to account for the effects of turbulence. These turbulence models fall into two main categories: models based on turbulent viscosity (k-ε, k-ω) and models based on Reynolds stress (Reynolds-Stress Transport (RST)). The numerical simulation does not seek to determine the instantaneous turbulent flow, but simply to obtain information about its mean behavior. The choice of approach depends on the desired level of detail and the available computing resources for studying and solving complex flows.

1.3.3 Turbulent Viscosity

As we mentioned, when we simulate turbulent flows, we use a term called '**turbulent viscosity**.' To better understand its importance, consider this statement: "The main parameter related to turbulence in rivers is the **eddy viscosity**, which is used to model a turbulent flow." (R.Absi, 2021) [3], But what does that term mean, and why is it important in simulating turbulence?

Turbulent viscosity is a concept used in fluid dynamics to quantify how effectively a fluid resists turbulent and chaotic movements and how energy dissipates in turbulent flow. The introduction of the turbulent viscosity parameter based on the Boussinesq hypothesis (1877), helps solve the challenge of modeling turbulent flows. This approach suggests establishing a linear connection between turbulent stresses and the average velocity gradient.

According to Pope (2000) [4], turbulent viscosity is not a property of the fluid itself but rather a characteristic of the turbulent flow field. It is defined as the combination of molecular viscosity which is an inherent property of the fluid, and turbulent viscosity a modeling concept, this definition is crucial for comprehending how turbulent flow behaves and how energy dissipates.

Here are the most commonly used turbulence models

- Spalart-Allmaras model
- Standard k-ε model
- RNG k-ε model
- Realizable k-ε model
- Standard k-ω model
- k-ω SST (Shear-Stress Transport) model
- Reynolds stress model (RSM)

1.4 Flow over Rough Surfaces

1.4.1 Effects of Roughness on Flow

The term "flow over a rough surface" pertains to any fluid motion transpiring above a surface characterized by roughness. The surface's degree of roughness represents a critical factor that distinctly impacts the character of the surface, and this impact is contingent upon several factors, namely, the mean height of the roughness elements, deviations from the mean height, and the shape and spatial distribution of these roughness features. The presence of roughness affects the fluid flow by creating disturbances and altering the boundary layer, which can lead to changes in friction, turbulence, and heat transfer characteristics of the flow.

The effects of roughness on a flow are primarily observed within the boundary layer, especially in the viscous sublayer near the rough surface. It is in this region that roughness disrupts the fluid velocity, creating local variations, turbulence zones, and small-scale vortices. As one moves away from the surface, the effects of roughness become less significant, and the flow regains a more regular character. Understanding the dynamics of the boundary layer and the viscous sublayer is crucial for assessing how roughness impacts drag, energy dissipation, and other aspects of the flow.

1.4.2 History of Roughness Studies

The history of studying roughness dates back to ancient times when early investigations were primarily conducted by hydraulic engineers. They initiated the examination of how roughness affects fluid flows. These pioneering studies laid the foundation for a better understanding of the influence of roughness on fluid flows and greatly contributed to our current knowledge of this interaction.

In 1883, Osborne Reynolds published a significant paper in which he investigated the effects of roughness on the transition from laminar to turbulent flow. This study is closely associated with the concept of the Reynolds number, a crucial parameter for characterizing flow behavior. Reynolds conducted experiments with flows inside pipes to comprehend how wall roughness affects the transition from laminar to turbulent flow. This research laid the groundwork for our understanding of turbulent flows [5].

In 1904, Ludwig Prandtl published a notable paper in which he developed a theory of turbulent boundary layers that accounts for roughness. The boundary layer is the region near the surface of an object or wall where flow velocity significantly decreases due to viscous friction.

Prandtl elaborated on theories concerning turbulent boundary layers, taking into account wall roughness and how it influences flow properties [6].

In 1933, Albert Nikuradse published a paper presenting a technique for quantifying the equivalent roughness, a standardized metric used to describe surface roughness. Nikuradse's research significantly influenced the development of measurement standards for surface roughness in fluid mechanics experiments, ultimately deepening our comprehension of the impact of roughness on fluid flows [7].

1.4.3 Equivalent Roughness (K_s)

Equivalent sand-grain roughness (k_s) is a parameter used to describe the roughness of surfaces that deviate from the idealized uniform sand-grain roughness. It represents a characteristic roughness height that simplifies the analysis of flows over complex, irregular, or non-uniform rough surfaces. When introduced into calculations, k_s provides results that are consistent with the behavior of flows over idealized rough surfaces, particularly in the fully rough flow regime, such as those observed in Nikuradse's experiments. It serves as a useful tool for characterizing and modeling the impact of roughness on fluid flow.

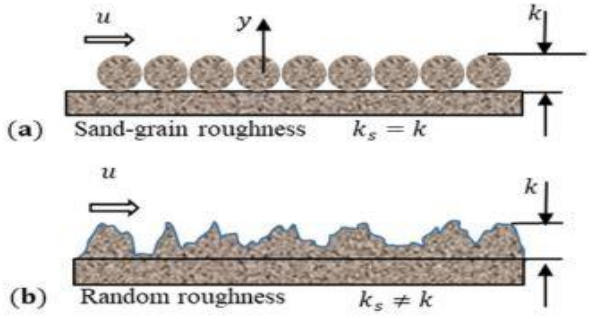

Figure 1.1: Equivalent sand-grain roughness.

1.4.4 Roughness Flow Regimes

The presence of roughness alters the law of the wall applied to the viscous sublayer. In this context, we introduce a new parameter, known as the 'roughness Reynolds number,' denoted as ks+.

$$k_s^+ = \frac{K_s \times U_*}{\nu} \tag{1.1}$$

The beds can then be classified into three categories according to this roughness Reynolds number [8]:

- **Hydraulically smooth beds: $k_s^+ < 5$**: the roughness elements are entirely embedded in the viscous sublayer,
- **Transition beds: $5 < k_s^+ < 70$:** the influence of the surface roughness is complex. In this regime, both the Reynolds number and relative roughness influence the skin friction and drag coefficients. This means that both viscous and pressure forces influence the skin friction and drag coefficient. The Transitionally rough regime is associated with the reduced sublayer thickness.

- **Hydraulically rough beds $k_s^+ > 70$:** the rough elements protrude into the fully turbulent region shifting the logarithmic profile downwards. In this flow regime, the viscous sublayer is entirely destroyed by the large turbulence mixing caused by roughness elements. The friction drag significantly increases due to pressure force on the roughness and is independent of the viscous effect (Reynolds number). The pressure loss becomes independent of the molecular viscosity of fluid and velocity when roughness elements intrude viscous sublayer

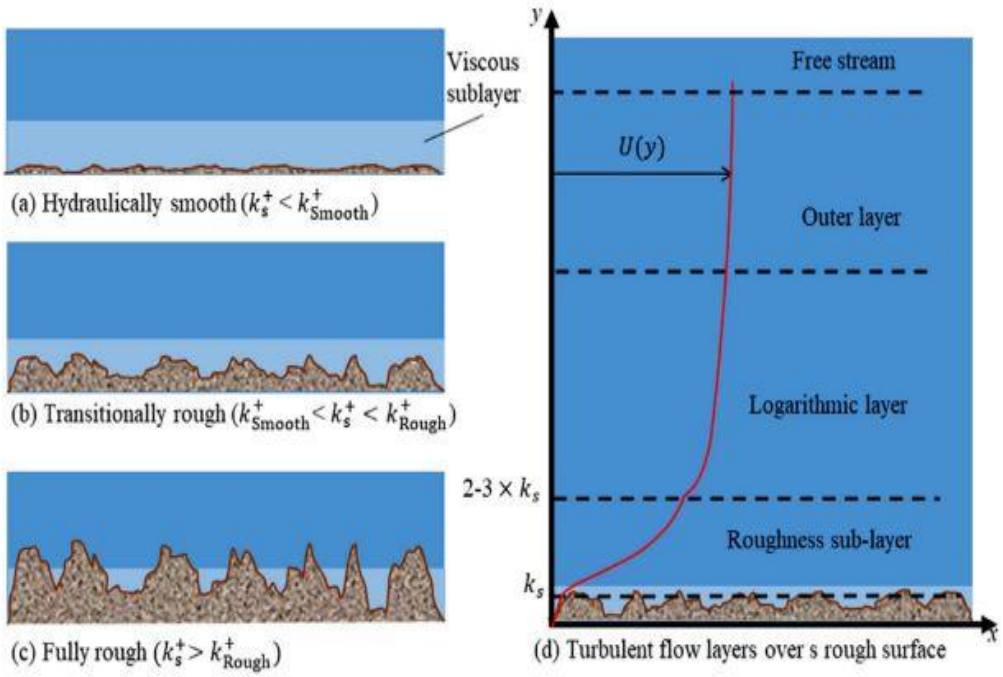

Figure 1.2 :Turbulent flows over rough surfaces; (a) hydraulically smooth regime with roughness embedded under the viscous sublayer, (b) transitionally rough regime with partially destroyed viscous sublayer, (c) fully rough regime with completely destroyed viscous sublayer, (d) schematic of velocity profile U(y) over roughness with the indication of rough-ness sublayer, logarithmic layer and outer layer.

1.5 Turbulent Boundary Layers

A turbulent boundary layer is a thin layer of fluid that forms near the surface of a solid object (such as a wall) when a fluid flows over that object. This boundary layer is characterized by irregular, chaotic fluid motion and is typically found in the transition from laminar (smooth and orderly) flow to turbulent (disordered and chaotic) flow.

1.5.1 Turbulent Boundary Layer over Smooth and Rough Surfaces

A turbulent boundary layer can form along both smooth and rough surfaces. However, the specific characteristics of the turbulent boundary layer and when it becomes turbulent can vary depending on the roughness of the surface and the flow conditions.

On a smooth surface, the boundary layer usually becomes turbulent at a set distance from the start. On the other hand, on a rough surface, the transition to turbulence can occur earlier due to the flow disturbance caused by the roughness. The features of the turbulent boundary layer change based on how rough the surface is.

The thickness of the boundary layer is typically greater in flow over a rough surface compared to a smooth surface, the reason is that the surface roughness disrupts the flow and creates turbulence, which leads to a thicker boundary layer.

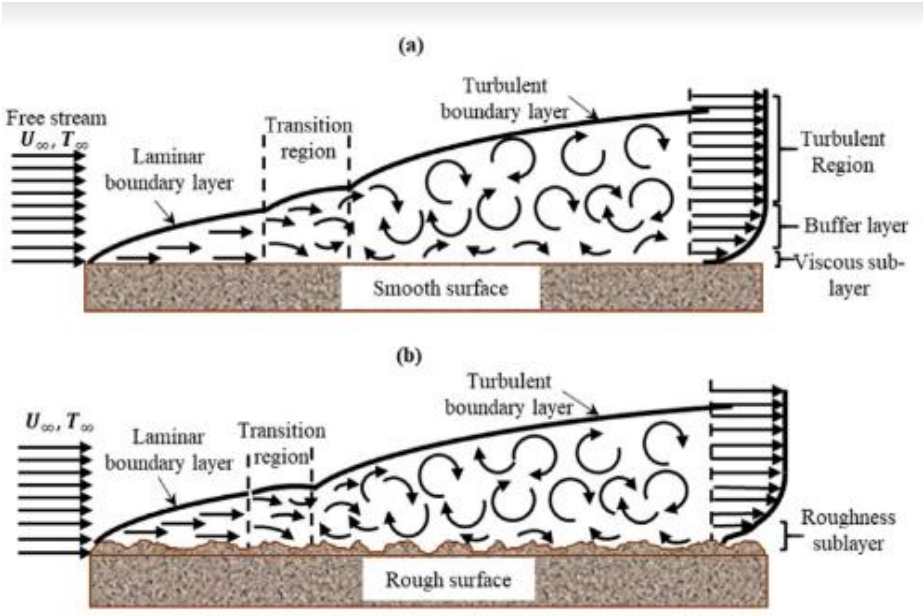

Figure 1.3 :Boundary layer flows over (a) smooth and (b) rough surfaces.

1.5.2 Structure of the Turbulent Boundary Layer

In the study of turbulent boundary layers, the decomposition of the boundary layer into inner and outer regions is a fundamental concept, and it helps in understanding the different flow characteristics within these regions.

1.5.2 .1 Inner Region (ξ < 0.2)

(where $\xi = y/h$ is the ratio of the distance from the bed y to flow depth h), this is the region of the boundary layer that is very close to the wall, typically within the first 20% of the boundary layer thickness [9]. The flow in this region is characterized by high levels of turbulence, strong velocity gradients, and significant viscous effects and velocity is zero at the wall.

Inner Sub-Layers: Within the inner region Using a dimensionless parameter known as the "inner coordinate"

$$y^+ = \frac{y \times u_*}{\nu} \tag{1.2}$$

where u_* represents the friction velocity and ν is the kinematic viscosity, three distinct zones within the near-wall layer are typically distinguished, these are the viscous sub-layer, buffer layer, and overlap layer.

- **Viscous Sub-Layer:** This is the layer very close to the wall, where viscous effects dominate. The velocity profile is approximately linear, and it's important for understanding wall shear stress.
- **Buffer Layer:** Just above the viscous sub-layer, the buffer layer is characterized by the transition from the linear velocity profile to a logarithmic one. This is where the effects of turbulence start to become significant.
- **Log law layer:** This is the region above the buffer layer but still within the inner region. It's where the logarithmic velocity profile dominates, and the turbulence intensity is highest.

1.5.2.2 Outer Region (ξ > 0.2)

This is the region farther away from the wall, typically beyond the first 20% of the boundary layer thickness. In this region, the flow is less affected by viscous effects and has a more uniform velocity profile. Turbulence in this region is less intense and is dominated by large eddies.

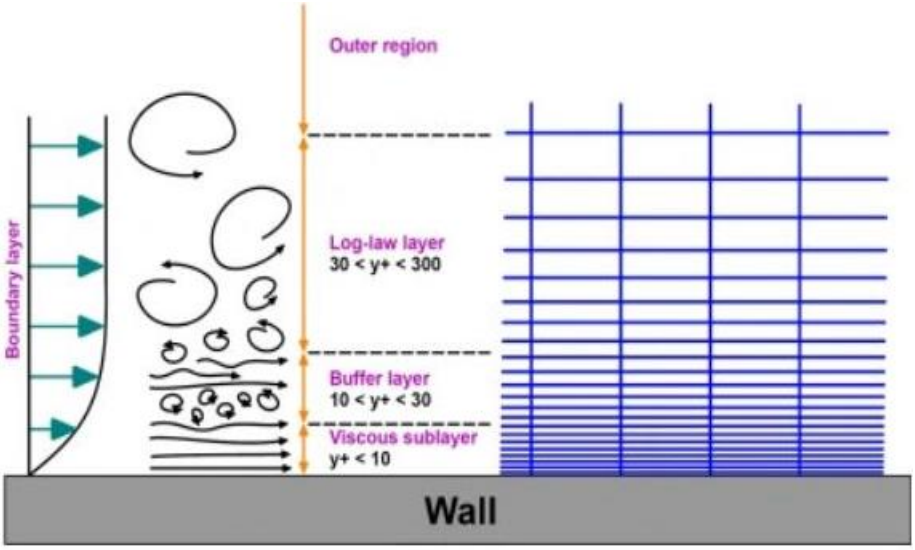

Figure 1.4 :Turbulent boundary layer structures

1.6 Estimation of Wall Parameters

1.6.1 Estimation Methods

Several parameters associated with the boundary layer, they can be estimated in different ways, either directly or indirectly, depending on the specific application context and the available data. The choice between these two methods depends on the specific context of the application and the available resources.

If precision is crucial and you have the financial and technical means, direct estimation may be preferred. However, indirect estimation may be more appropriate if budget constraints or technical limitations are a key factor.

Here is a simplified explanation of both methods:

1.6.1.1 Direct Estimation

This method involves measuring wall parameters using a suitable measuring device, like a pressure sensor or a velocity measurement tool. This approach is the most accurate but can be expensive and challenging to implement.

1.6.1.2 Indirect Estimation

Indirect estimation means estimating wall parameters based on available information, such as fluid properties, wall geometry, or numerical simulation results. While it's less precise than direct estimation, this method is easier to implement and can be sufficient for many applications.

1.6.2 Boundary Layer Thickness (δ)

Boundary Layer Thickness (δ) is a measure of how thick this layer is. It is typically defined as the distance from the solid boundary at which the velocity of the fluid reaches 99% of the free-stream velocity. Boundary layer thickness is essential for understanding how the velocity profile changes from the wall to the outer flow region.

The boundary layer thickness (δ) is typically measured experimentally using techniques such as Laser Doppler Velocimetry (LDV) or pressure sensors.

In some cases, the thickness of the boundary layer can be estimated by using numerical Methods such as the logarithmic velocity profile

steps to estimate the boundary layer thickness (δ) from the logarithmic velocity profile using the law of the wall:

- **Collect Velocity Data:** Velocity data is gathered at various distances from the wall in the flow direction. This data is essential for understanding the velocity profile within the boundary layer.
- **Identify the Logarithmic Region:** The next step involves identifying the region in the velocity profile where the behavior is linear when plotted on a logarithmic graph. This linear region is crucial for applying the law of the wall method.
- **Perform Linear Regression:** In the identified logarithmic region, a linear regression is conducted to determine the von Kármán constant, κ. This statistical method quantifies the relationship between fluid velocity and the distance from the wall.
- **Estimate Boundary Layer Thickness (δ):** With the von Kármán constant obtained through linear regression, the boundary layer thickness can be estimated at a specific distance from the wall within the boundary layer. This estimation involves a mathematical relationship that considers the fluid velocity at that distance and the reference velocity of the fluid.

1.6.3 Friction Velocity (u_*)

Friction Velocity (U_*) is a characteristic velocity scale for the flow in the boundary layer. It is related to the shear stress at the wall. The value of U_* is critical for characterizing the velocity distribution near the wall.

1.6.3.1 Average Estimations of u_* (Friction Velocity)

To estimate the average friction velocity in uniform turbulent flows with an open channel slope equal to the bed slope we use this equation:

$$u_* = \sqrt{g \times R_h \times I_s} \tag{1.3}$$

g: represents the acceleration due to gravity, R_h: hydraulic radius of the channel and I_s: free surface slope. This method provides an overall estimation of friction velocity, while other methods typically estimate a local value for friction velocity.

1.6.3.2 Estimating u_* through measurement

The friction velocity (u_*) of a fluid close to a surface can be estimated by measuring the wall shear stress (τ_p) and the fluid's density (ρ). This formula is used to make this estimation

$$u_* = \sqrt{\frac{\tau_p}{\rho}} \tag{1.4}$$

1.6.4 Friction Reynolds Number (Re_*)

Friction Reynolds Number (Re_*) is a dimensionless quantity used to describe the flow regime in the boundary layer. Re_* helps classify flows as laminar or turbulent within the boundary layer.

Estimating the friction Reynolds number (Re_*) involves measuring the wall shear stress τ_p, knowing the fluid's properties (density ρ, kinematic viscosity ν) calculating the friction velocity, specifying the distance from the surface (h), and using this equation:

$$Re_* = \frac{h \times u_*}{\nu} \tag{1.5}$$

1.6.5 Roughness Parameters (k_s, y_0)

The estimation of roughness parameters k_s (equivalent sand grain roughness) and y_0 (roughness length) characterizing the wall in turbulent flows can be achieved through various methods. One of the most direct methods involves linear regression on the dimensionless velocity profile using

$$u^+ = \frac{U}{u_*} \tag{1.6}$$

where u^+ is a variable used to describe the dimensionless velocity profile of turbulent flow near the wall of a pipe or channel

In logarithmic coordinates [4][10] providing access to k_s and y_0 through the slope and intercept of the relationship:

$$u^+ = \frac{1}{K}\ln\left(\frac{y}{k_s}\right) + b \tag{1.7}$$

κ is the von Kármán constant.

Here is how to implement this method in detail:

- Measure the velocity profile at different heights (y) near the wall.
- Plot u^+= f(ln(y)).
- Perform a linear regression on the logarithmic part:
- Use specialized software to conduct a linear regression on this part of the curve, obtaining an equation in the form of $u^+ = a \times \ln(y) + b$

Deduce k_s and y_0:

- The slope of the line (a) is related to k_s: $K_s = \frac{-1}{a}$
- The y-intercept (b) is related to y0: $y_0 = u_* \times e^b$

1.7 Logarithmic Velocity Laws

1.7.1 On Smooth and Rough Surfaces

Among the various velocity profile models available in the literature, the well-known and widely applied equations are selected for the corresponding layer/region:

- **Viscous sub layer**

In the viscous (laminar) sublayer where y^+ <5, which is attached to the surface the mean velocity can be expressed with a linear law as:

$$u^+ = y^+ \tag{1.8}$$

- **The log layer**

law of the wall or log-law [11] where y^+ >30 :

$$u^+ = \frac{1}{K}\ln(y^+) + A \tag{1.9}$$

Where κ = 0.412 (Von Karman constant) and A = 5.29 (a constant).

Regarding the transitionally and completely rough beds in open channel fows [11] proposed a roughness shift ΔU^+

$$u^+ = \frac{1}{k}\ln(y^+) + A - \Delta U^+ \tag{1.10}$$

ΔU^+ increases with increasing roughness Reynolds number k_s^+.

The values of ΔU^+ range between 0 (smooth bed) and 7.4–7.6 (fully rough bed) For transitionally rough beds, ΔU^+ values are reported between 3.5 and 6

- **The outer layer**

The outer region (where y/h > 0.2), is also called the defect layer the velocity distribution deviates from the log-law and follows a parabolic function, including the wake parameter Π. In this region, the log-law with Coles' wake function for hydraulically smooth beds is written as:

$$u^+ = \frac{1}{\kappa}\, ln(y^+) + A + \frac{\Pi}{\kappa} w\left(\frac{y}{\delta}\right) \tag{1.11}$$

with:

$$w\left(\frac{y}{\delta}\right) = 2sin^2\left(\frac{\pi z}{2\delta}\right) \tag{1.12}$$

1.7.2 In Narrow and Wide Channels

The lateral confinement governs significant physical phenomena that impact the longitudinal mean velocity profile [12] [13] It is defined by the transverse shape factor Ar_y

$$A_{r_y} = \frac{b}{h} \tag{1.13}$$

With b: characteristic width of the channel [m] and h: the water depth [m].

The index 'y' indicates the direction of confinement.

In order to differentiate between a wide channel and a narrow channel, Nezu (1985) [14] classified using experimental measurements the second type Prandtl secondary currents based on the transverse shape factor Ar_y, which represents the aspect ratio, into two types of channels: wide channel and Narrow channel

- **In wide channels,** when $\mathbf{Ar_y > 5}$, corner secondary currents are present and located on both sides of the center over a distance:

$$\left|\frac{y}{h}\right| < \frac{\frac{B}{h} - 5}{2} \tag{1.14}$$

The vertical profile of longitudinal mean velocity encountered remains a logarithmic-type vertical profile, except at the edges, with the maximum flow velocity occurring at the free surface.

- **In narrow channels**, when $\mathbf{Ar_y \leq 5}$ (experimentally estimated critical value), a **dip phenomenon** occurs. This phenomenon alters the vertical profile of longitudinal mean velocity, transitioning from a logarithmic law to a parabolic law and the position of the maximum velocity is located below the free surface. Additionally, if the channel bed is heterogeneous in roughness [15] the entire flow becomes three-dimensional. The dip phenomenon represents a significant change in velocity distribution and is associated with the channel's shape, particularly in narrow channels.

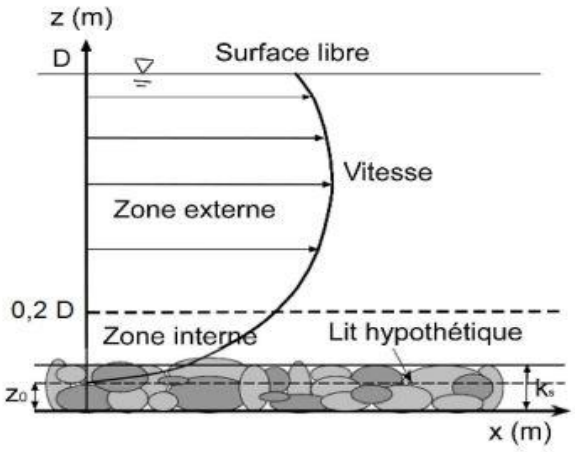

Figure 1.5 :Schematic representation of the vertical profile of mean longitudinal velocity U in the presence of secondary currents in a narrow channel (Bonakdari et al., 2008)

ξdip is a variable that represents the position of the maximum velocity on the vertical profile of the mean longitudinal velocity in a narrow channel. It is defined as the ratio of the distance from the maximum velocity to the free surface of the fluid to the depth of the channel.

The authors (Wang et al., 2001) [16] found that there was no direct physical relationship between the shape ratio (Ar_y) and the position ξdip. In order to address this, they developed an empirical relationship based on experimental data for when Ar_y is less than 5.2.

The empirical relationship is given by the following equation:

$$\xi\text{dip} = 0.44 + 0.106A_{r_y} + 0.05\sin(\frac{2\pi}{2.6A_{r_y}}) \quad (1.15)$$

This equation allows for the calculation of the ξdip position as a function of Ar_y within this specific range of values. However, it's important to note that this relationship is empirical, meaning it is based on experimental observations rather than fundamental physical principles, and it may not be applicable outside the range of $Ar_y < 5.2$ or in different conditions.

1.8 Conclusion

In conclusion, this literature review has provided an overview of the key concepts associated with turbulent free-surface flows on smooth and rough beds. Key notions such as flow regimes, turbulent boundary layer structure, and the estimation of wall parameters have been addressed. This review highlights the complexity of these flows and the necessity for further research through in-depth experimental and numerical studies, particularly on practical cases of rough riverbeds. The objective is to enhance the understanding and modeling of turbulent flows over rough substrates, considering the combined effects of roughness and three-dimensionality.

Chapter 2: Literature Review - Roughness Effects on Turbulent Velocity Profiles in Free Surface Flows

2.1. History Overview: The Influence of Roughness on Turbulent Flows

2.1.1 Early Studies on Turbulent Flows

In the early 20th century, researchers began to explore the complex behaviour of fluids flowing over several types of surfaces. Ludwig Prandtl In 1904 achieved a significant milestone; he is the one who first mentioned the notion of the boundary layer [17] [18]. This boundary layer is a critical region near a solid boundary where the behaviour of the fluid changes from laminar to turbulent flow. Prandtl's work laid the foundation for the understanding of turbulent flows over various surfaces.

2.1.2 Nikuradse's Experiments (1933) and CLAUSER, Francis H (1954)

In 1933, Johann Nikuradse [7] [19] made a breakthrough in the study of turbulent flows over rough boundaries. He conducted extensive experiments using sand grains to explore how fluids behave near rough walls, which involved measuring the velocity profiles in turbulent boundary layers. Nikuradse's experiments provided intriguing insights into the effects of roughness elements on flow patterns. Moreover, he discovered that the logarithmic law remains valid above roughness but with a shift (ΔU^+) [20], connected to what we call the equivalent height of sand grains, often represented a (h_s).

In 1954, Francis H. Clauser [20] [50] introduced a logarithmic velocity distribution model for turbulent flow over rough surfaces. According to his work, this model can be expressed as follows:

$$U^+ = \frac{1}{K}\ln(y^+) + C - \Delta u^+ \qquad (2.1)$$

$$U^+ = \frac{u}{u_*} \quad ; \quad y^+ = \frac{y\,u_*}{\nu} \quad ; C = 5.5 \quad ; \quad k = 0.40$$

Here, C represents the intercept for smooth walls, and k stands for the von Karman constant. Clauser [50] also emphasized that the roughness function ΔU^+ is solely dependent on the roughness Reynolds number h_s^+ with $h_s{}^+ = \frac{h_s\,u_*}{\nu}$ [5] [36].

The relationship between the velocity profile U^+ and the dimensionless height ${h_s}^+$ is expressed as [7] [19] [20]:

$$U^+ = \frac{1}{k} \ln\left(\frac{y^+}{{h_s}^+}\right) + B \tag{2.2}$$

where $1 < {h_s}^+ < 3.5$; $B = 5.5 + \frac{1}{k} \ln({h_s}^+)$

$3.5 < {h_s}^+ < 7$; $B = 6.59 + 1.52 \ln({h_s}^+)$

$7 < {h_s}^+ < 14$; $B = 9.59$

$14 < {h_s}^+ < 68$; $B = 11.5 - 0.7 \ln({h_s}^+)$

$68 < {h_s}^+$; $B = 8.48$

The shift (ΔU^+) can be represented more concisely according to Grigson's formulation [20] [21] as follows:

$$\Delta U^+ = \frac{1}{k} \ln\left(1 + \frac{{h_s}^+}{\exp(3.25k)}\right) \tag{2.3}$$

2.1.3 von-Karman Constant (κ)

Nikuradse's experiments [19] also led to the identification of the von-Karman constant (κ) [22] [23], a fundamental constant in the study of turbulent flows. The von-Karman constant represents the slope of the time-averaged streamwise velocity profile in a semi-logarithmic scale. Remarkably, this constant was found to have the same value for both smooth and rough walls, regardless of the type and size of roughness elements.

The streamwise velocity profile in a turbulent boundary layer can be expressed as:

$$\frac{u}{u^*} = A \ln\left(\frac{z u_*}{\nu}\right) + B \tag{2.4}$$

The A is represented by $1/\kappa$, where κ symbolizes the universal von Karman constant, which remains unaffected by the wall's nature, whether it is smooth or rough. Meanwhile, B represents a constant whose numerical value is contingent upon the characteristics of the wall surface, as observed in Schlichting's research in 1968 [24] .

Based on Nikuradse's experiments [7] [19] on hydraulically "smooth" pipe flow in 1932, the specific values of A and B were determined to be 2.5 and 5.5, respectively [20].

2.1.4 Modifications to Van Driest Damping Function

In subsequent years, researchers sought to improve the van Driest damping function (1954) [53] to account for the impact of roughness on velocity profiles. Per-Age Krogstad made one notable contribution [25], he came up with a new way to make turbulent shear forces near the wall stronger. Instead of shifting the wall's position, he changed the level of viscous damping. What is interesting is that when dealing with very rough surfaces, there's a middle layer called an intermediate logarithmic layer. This layer connects the fully turbulent logarithmic region to the viscous sublayer. Understanding this region is essential when aiming to determine the skin friction coefficient through the alignment of velocity profiles with the law of the wall.

2.1.5 Drag-Based Models

As research progressed, an alternative approach to represent the effects of roughness on turbulent flows over rough beds emerged - the "drag-based models " [26] [27]. These models partition the total shear stress into two components: one component is associated with the fluid motion (modelled using an eddy-viscosity model), and the other component results from the drag force acting on the roughness elements.

2.1.6 Double-Averaged N-S Equations

In more recent years, researchers have explored the use of "double-averaged Navier-Stokes equations" [28] [29] to model the effect of roughness on turbulent flows. These equations consider the drag force, form-induced momentum flux, and the interaction of turbulence with roughness elements at different spatial scales.

2.1.7 Advancements in Computational Fluid Dynamics (CFD)

In the modern era, with the advent of sophisticated computational fluid dynamics (CFD) techniques [30] [31], researchers have gained the ability to simulate turbulent flows over rough beds more accurately. Numerical simulations using CFD have become an essential tool in investigating the complex interaction between turbulence and roughness elements.

These simulations [32] have been instrumental in revealing intricate details of flow behaviour near rough boundaries. By simulating flows over various roughness configurations and scales, researchers have been able to validate and improve drag-based models and other representations of roughness effects.

2.2. Velocity Distribution in Fully Developed Turbulent Shear Layers in Free Surface Flows

2.2.1 For Smooth Surfaces

2.2.1.1 Inner Region

In the inner region (Cebeci and Smith 1974) [34], the mean velocities are influenced by several factors including the wall shear stress, wall roughness, distance from the wall, fluid density, and viscosity [33].

In this context, the viscous sublayer is important. According to Klebanoff's work [35] in 1954, the total shear stress at a small distance from the wall remains constant and equals the wall shear stress, denoted as τ_0.

When we integrate Newton's law of viscosity $\left(\tau = \mu\frac{du}{dz}, \text{with } \tau = \tau_0\right)$, we obtain the following velocity distribution equation [19]:

$$\frac{u}{u_*} = \frac{u_* z}{\nu} \tag{2.5}$$

Where u_* represents shear velocity, ν represents kinematic viscosity, and z denotes the distance measured from the solid boundary.

In the fully turbulent part, we refer to the logarithmic velocity distribution equation proposed by von Karman and Prandtl “Von Karman in 1930 [22] [23] and Prandtl in 1932 [36] [37]”, specifically the logarithmic portion of the "law of the wall":

$$\frac{u}{u_*} = A \ln\left(\frac{u_* z}{\nu}\right) + B \tag{2.6}$$

Here, $A = \frac{1}{\kappa}$ (κ is the universal von Karman constant [22] [23], unaffected by the wall type), and B represents a constant, and its value relies on the distinct characteristics of the wall's surface, as determined by Schlichting in 1968 [24].

2.2.1.2 Outer Region

In the outer region, velocities are primarily influenced by turbulent shearing [33] . This leads us to the velocity defect law [40], expressed as follows :

$$\frac{u_m - u}{u_*} = -\frac{1}{\kappa} \ln\left(\frac{z}{\delta}\right) \tag{2.7}$$

Here, u_m represents the maximum velocity within the distribution, δ indicates the boundary layer thickness, and κ equals 0.41. Originally, this equation was introduced by Prandtl in 1925 [36] and was intended to apply to both "smooth" and "rough" walls, as explained by Hinze in 1975 [43]. However, to better align with experimental data, a correction term with a value of 2.5 was later incorporated into the equation, as proposed by Clauser in 1956 [49].

In 1956, Coles expanded the law of the wall with an empirical correction function [33] .

$$\frac{u}{u_*} = \frac{1}{\kappa} \ln\frac{u_* z}{\nu} + B + \frac{\Pi}{\kappa} w\left(\frac{z}{\delta}\right) \tag{2.8}$$

Here the symbol Π represents the "profile" parameter, which has a defined value of 0.55 when κ equals 0.4 and B equals 5.1 [22] [23] , $w\left(\frac{z}{\delta}\right)$ is defined as $w\left(\frac{z}{\delta}\right) = 2\sin^2\left(\frac{\pi z}{2\delta}\right)$ and is referred to as the "law of the wake [24]." When we scribe the equation at the boundary layer's edge and subsequently deduct it, we arrive at the velocity-defect distribution established by Coles [38], can be expressed as [19]:

$$\frac{u_m - u}{u_*} = -\frac{1}{k} \ln\frac{z}{\delta} + \frac{\Pi}{k} 2\cos^2\left(\frac{\pi z}{2\delta}\right) \tag{2.9}$$

2.2.2 Rough Wall Velocity Distribution

Velocity distribution on rough surfaces is influenced by factors such as the grading, shape, and spacing of the roughness elements present [33]. In the context of studying velocity distribution in turbulent flows near rough boundaries, it is a frequent practice to utilize Nikuradse's (1933) expression [7] [19] [20] :

$$\frac{u}{u_*} = 2.5 \ln\left(\frac{z}{k_s}\right) + 8.5 \tag{2.10}$$

Where k_s is the original uniform sand grain roughness and z is the distance from the bottom of roughness elements .

For large Scale Roughness Viewpoint [33] (Bayazit 1976 [41]; Kamphuis 1974 [42]) estimated that the reference of the hypothetical bed (where mean velocity is zero) is between z = 0 and z = k (average height of roughness elements).

Cebeci and Smith 1974 [34] ; Hinze 1975 [43] they suggested that the velocity-defect law applies to rough surfaces. Zippe and Graf 1983 [44] they demonstrated that Coles's wake law effectively represents the turbulent velocity distribution in boundary layers with rough surfaces [19].

In 1962, Rotta [45] extended the law of the wall to the inner part of the boundary layer over a rough surface. He thought of roughness as if it were slowing down the flow in the viscous sublayer. This led him to create a formula for how the velocity behaves in that area [33].

$$\frac{u}{u_*} = \frac{1}{k} \ln\left(\frac{u_*(z + \Delta z)}{\nu}\right) + B - \frac{\Delta u}{u_*} \tag{2.11}$$

Δu represents velocity jump across the viscous sublayer due to Δz shift from the top of average roughness height, indicating the hypothetical bed level.

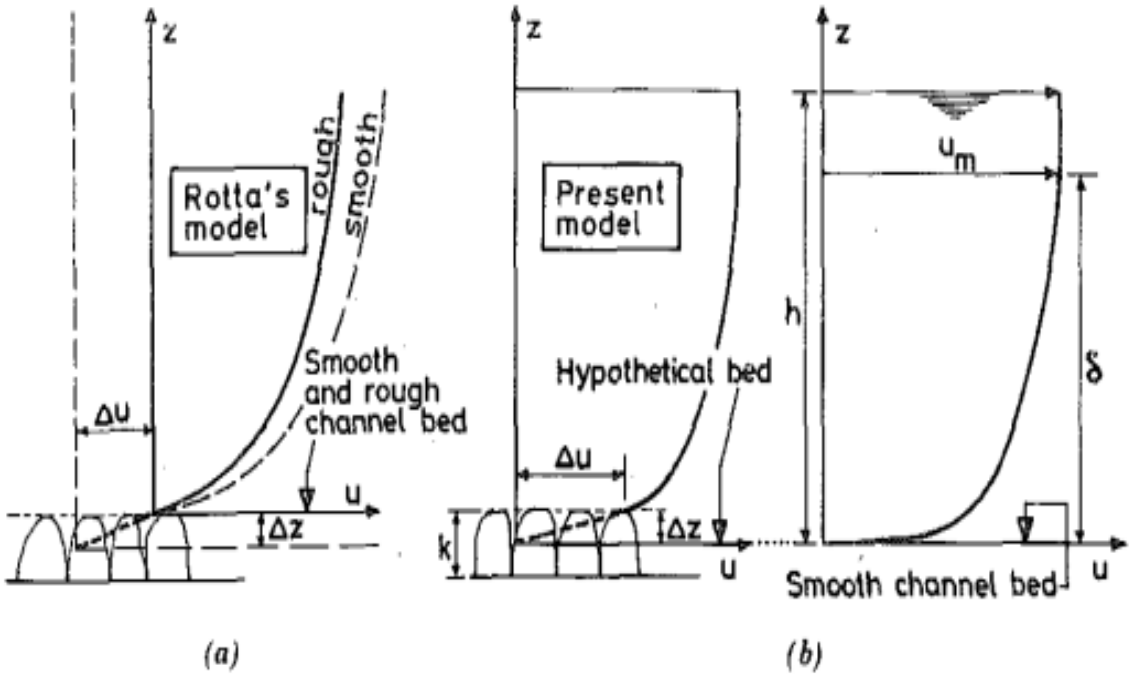

Figure 2.1: Definition Sketch of Rotta's model [33].

2.3. Review of relevant experimental studies on the impact of roughness on free surface flows in a chronological order

2.3.1 The work by M. Salih Kirkgoz [Nov 1, 1989]

2.3.1.1 Objective of the Study

In this investigation conducted by M. Salih Kirkgoz [33], the primary goal was to explore turbulent velocity profiles within open channel flows, comparing two scenarios: smooth and rough channel beds. To achieve this, a series of experiments were conducted in a laboratory channel with transparent walls. The aim was to investigate the impact of roughness on velocity profiles in open channel flow and to contrast these profiles with the established "law of the wall" and velocity-defect distribution models.

2.3.1.2 Experimental Setup

In pursuit of these objectives, a 12-meter-long, 0.3-meter-wide, and 0.3-meter-deep laboratory channel with glass walls was utilized. Velocity measurements were conducted using laser-doppler anemometry in a fully developed, rectangular, subcritical open channel flow. Experiments were conducted on both smooth and rough channel beds, featuring four different rough surfaces labelled as Rough 1, Rough 2, Rough 3, and Rough 4. These surfaces had aggregates of varying sizes, ranging from d90 = 2.36 mm to 20 mm. The research [33] sought to discern how diverse levels of roughness influence turbulent velocity profiles.

2.3.1.3 Results for Rough Surfaces

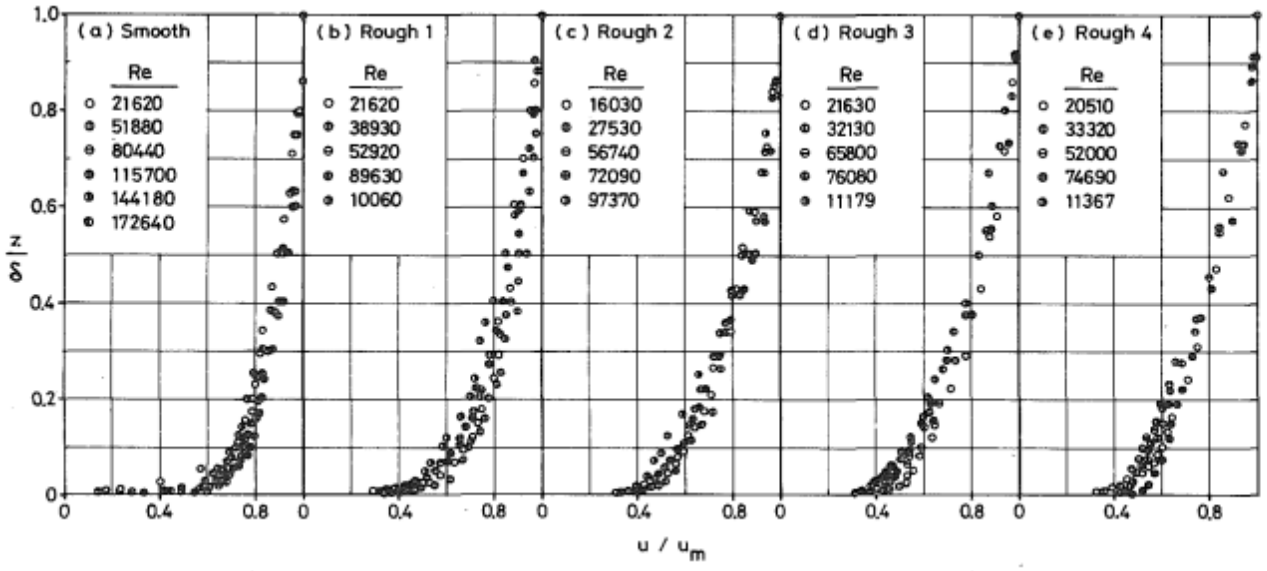

Figure 2.2: non-dimensional velocity distribution for smooth and rough surfaces [33].

This figure presents the measured velocity distributions for "smooth" and the four different "rough" surfaces. It is evident from this figure that the non-dimensional velocity distributions continuously, but slowly over time, diverge from near uniformity as the average uniform roughness height increases.

2.3.1.4 Determination of Shear Velocity

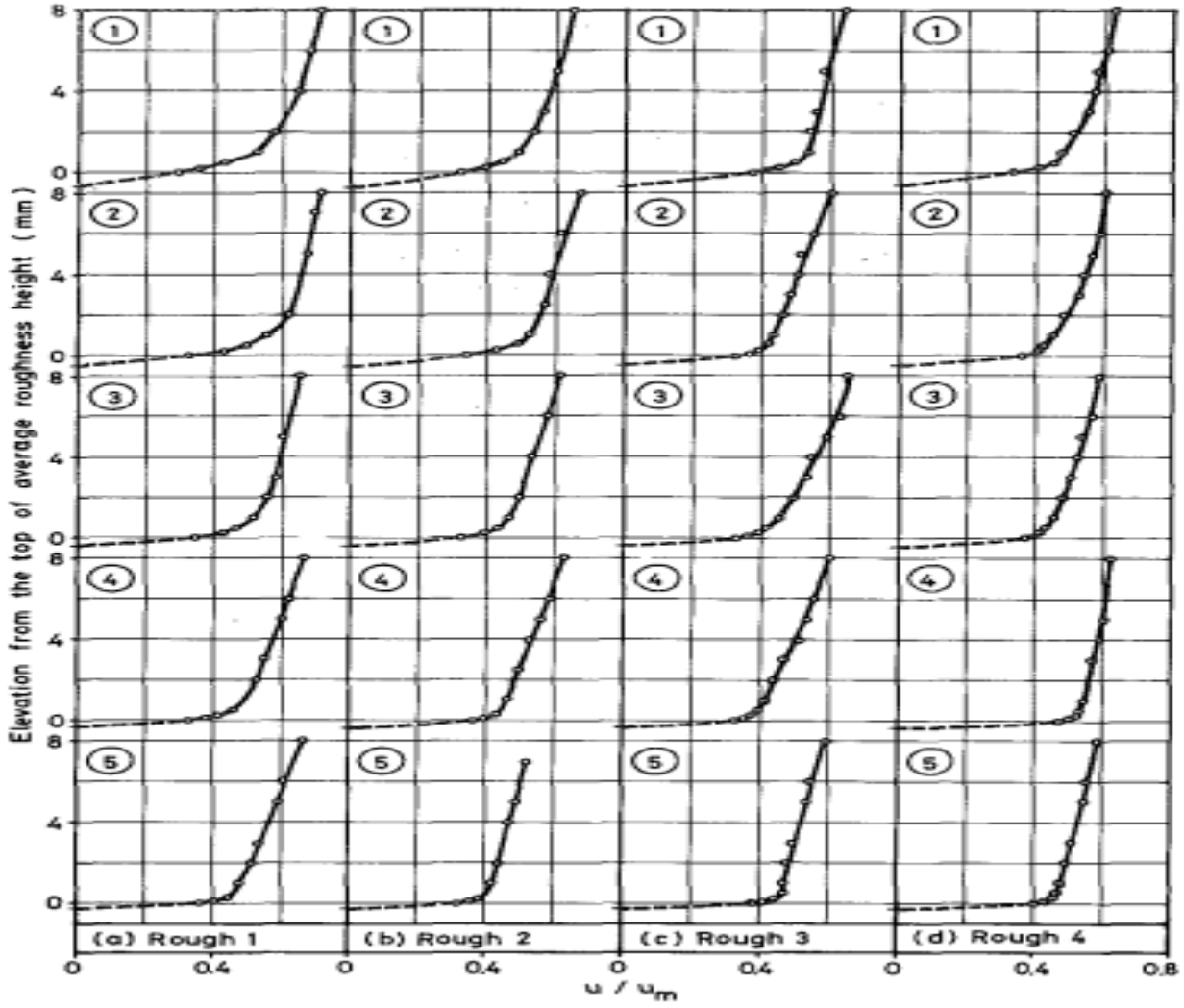

Figure 2.3: measured velocity distribution near different "rough" beds [33].

The study [33] also focused on determining the reference level where the mean velocity becomes zero near the wall. This reference level was shown to shift by an amount of Δz from the top of the average roughness level [45] [33], effectively altering the water depth to h + Δz. Notably, it was observed that the fictitious flow through this depth (Δz) exhibited laminar characteristics.

Additionally, Figure 2.3 demonstrates that Δz is more sensitive to the Reynolds number than to the range of values of the uniform roughness height used in this study.

2.3.1.5 Law-of-the-Wall Distribution

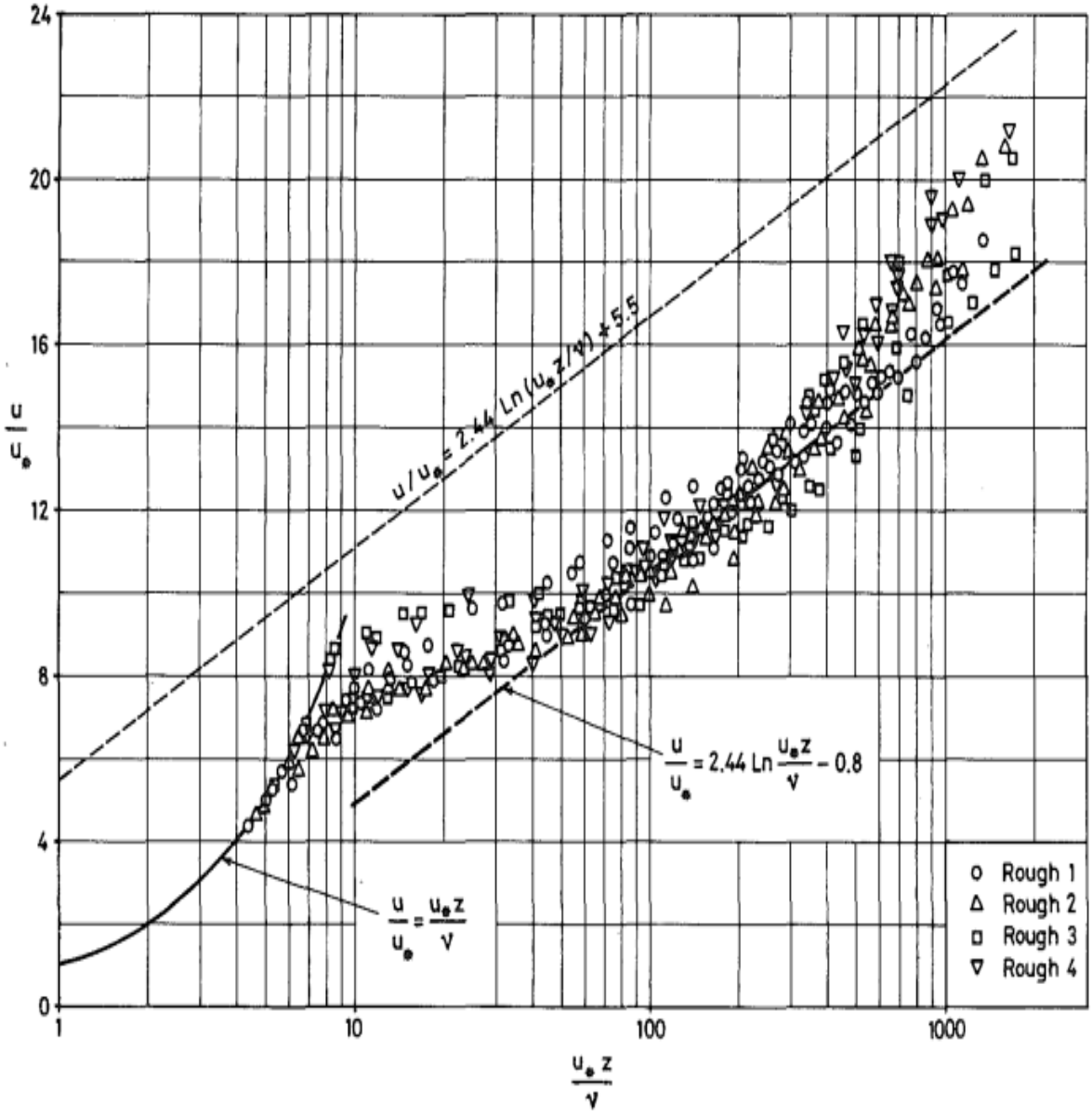

Figure 2.4: law of the wall distribution for rough beds [33]

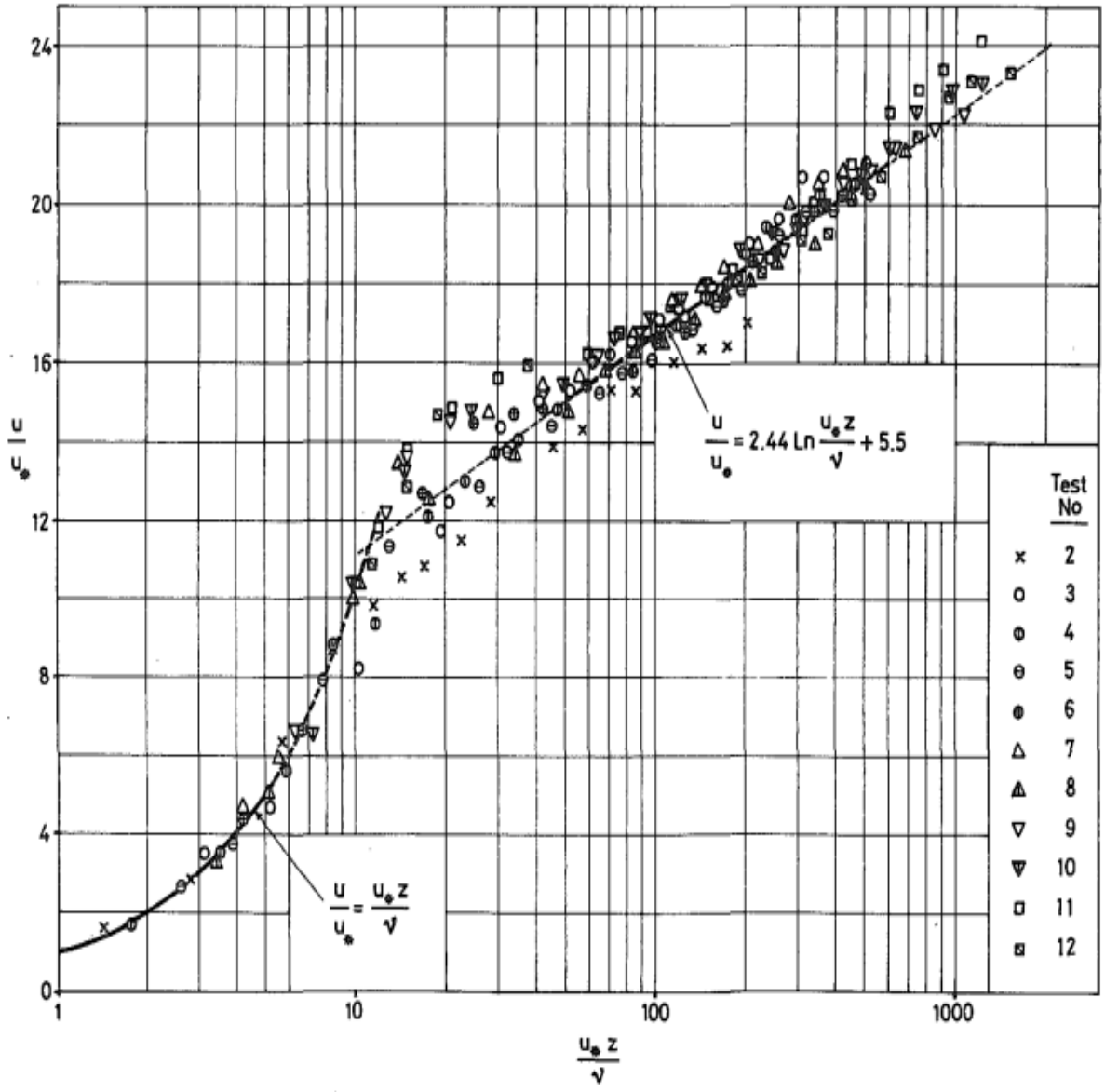

Figure 2.5: Law of the wall distribution for smooth bed [33].

The research also examined the "law-of-the-wall" distribution (fig 2.4) of mean velocities on rough surfaces, contrasting it with the corresponding distribution on a smooth wall (see Figure 2.5). A notable difference emerged: the values of u/u_* (nondimensional velocity) were notably lower for rough surfaces. This suggests that the flow dynamics on rough surfaces differ significantly from those on smooth surfaces.

2.3.1.6 Velocity-Defect Distribution

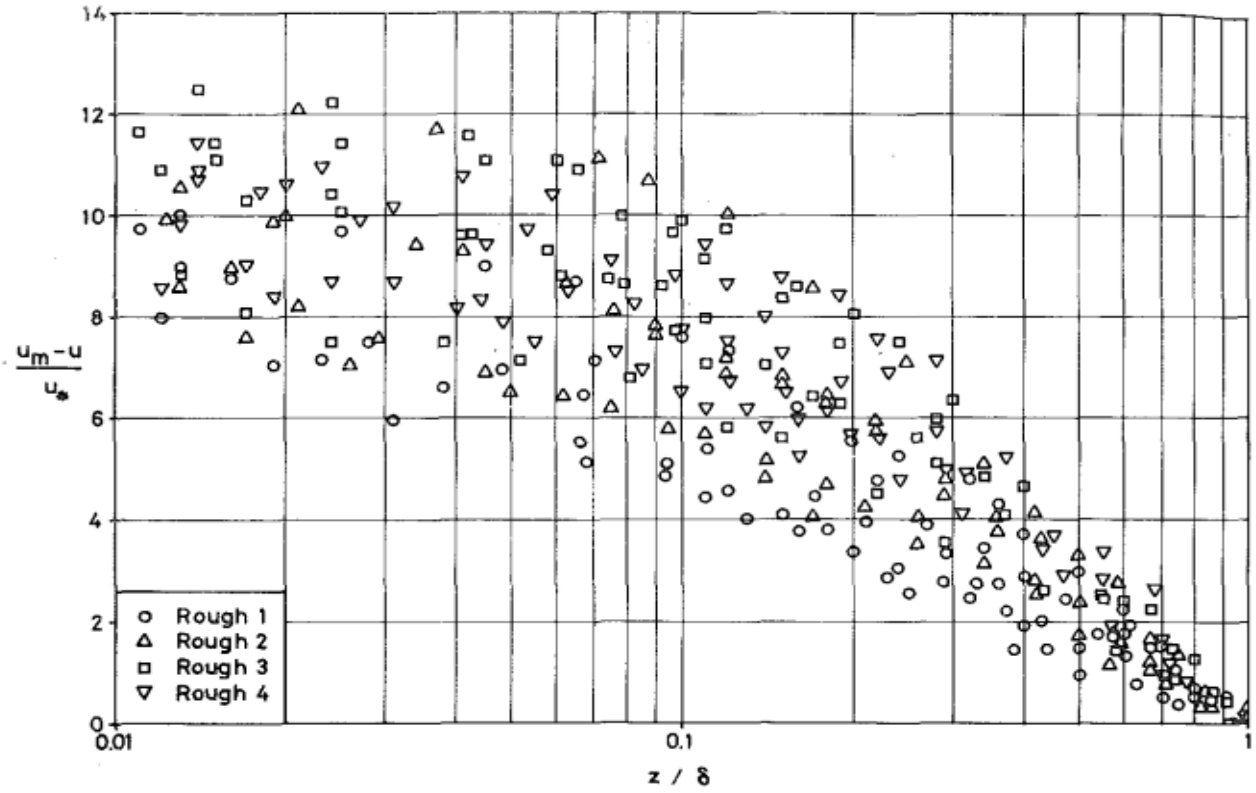

Figure 2.6: Velocity-Defect Distribution for "Rough" Beds [33]

Additionally, the study [33] delved into the velocity-defect distribution, showing that the outer region of the turbulent boundary layer is strongly influenced by wall roughness. This influence becomes more pronounced with increasing roughness height and Reynolds number, leading to a progressively non-uniform velocity distribution.

2.3.1.7 Conclusions

In conclusion, M. Salih Kirkgoz1's study [33] provided several key insights into mean velocity distributions in open channel flows with both smooth and rough boundaries. The key takeaways include the increasing non-uniformity of velocity distribution with rising uniform roughness height, the validation of the logarithmic law-of-the-wall distribution on smooth surfaces, and the sensitivity of reference shift to Reynolds number. The research also demonstrated that the "law-of-the-wall" model applied to velocity distribution on rough surfaces, although the velocity-defect distribution exhibited greater variability. These findings contribute to our understanding of turbulent flows in open channels, shedding light on the impact of roughness on velocity profiles.

2.3.2 The work by M. F. Tachie, D. J. Bergstrom, and R. Balachandar [2004]

2.3.2.1 Aims of the Study

The study conducted by Tachie, Bergstrom, and Balachandar [46] aims to investigate the effects of surface roughness on turbulent open channel flow. Specifically, the study focuses on how different surface geometries and Reynolds numbers influence key turbulence statistics, including Reynolds stresses, turbulence kinetic energy, turbulence diffusion, and the distribution of eddy viscosity and mixing length.

2.3.2.2 Experimental Setup and Procedure

The experimental setup involves an open channel flow with controlled variations in surface roughness [46]. The authors operated a Laser Doppler Anemometer (LDA) system with two components to collect velocity data. The rough surfaces consisted of wire mesh and sand grains with specific geometries. Measurements were obtained at various Reynolds numbers (Re) to capture a range of flow conditions.

These figures provide a visual representation of the experimental setup and initial results.

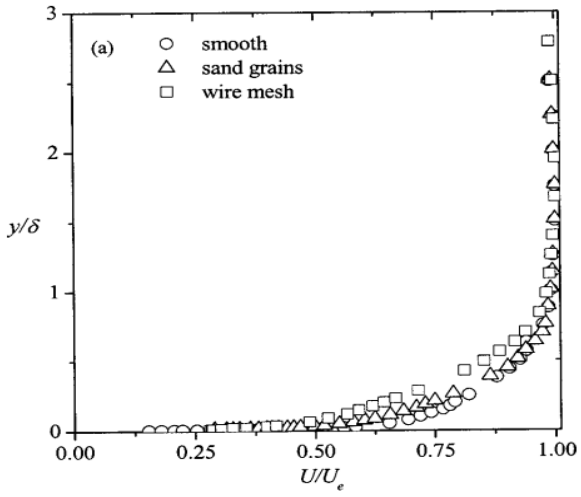

Figure 2.7a illustrates the roughness elements' geometries [46].

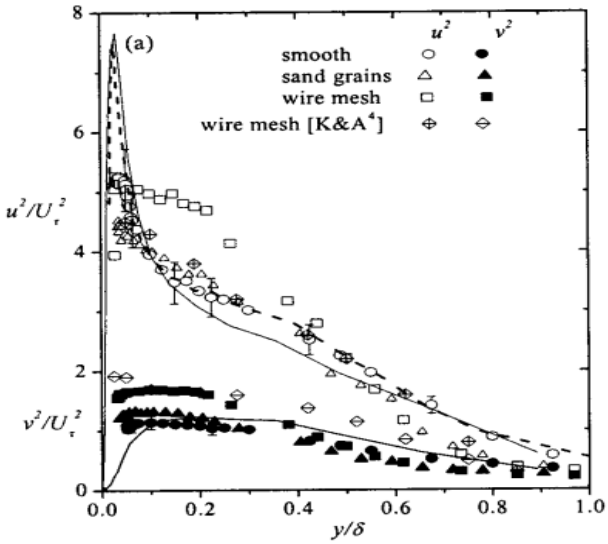

Figure 2.7b depicts the variations in Reynolds shear stress along the boundary layer for different surface roughness conditions (Tachie et al., 2002) [46] [47].

2.3.2.3 Results and Discussion

2.3.2.3.1 Influence of Surface Roughness on Reynolds Stresses and Turbulence Kinetic Energy:

Surface roughness significantly impacts the levels of Reynolds stresses and turbulence kinetic energy [46].

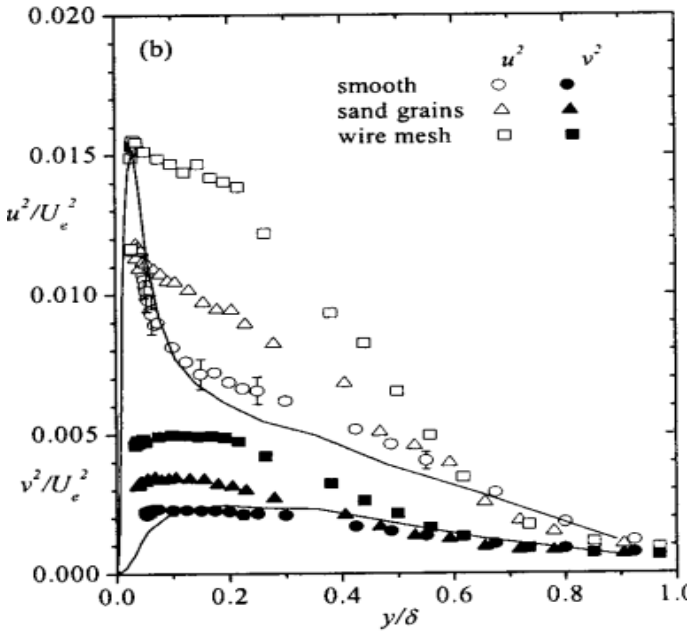

Figure 2.8 [46] shows the profiles of normalized turbulence kinetic energy and the uncertainty associated with these measurements (Tachie et al., 2002) [47]. This figure can be referenced when discussing how surface roughness alters the turbulence intensity distribution, especially in the vicinity of the wall. Surface roughness leads to higher turbulence kinetic energy levels, particularly in the inner region of the boundary layer.

2.3.2.3.2 Mixing Length and Eddy Viscosity:

Surface roughness also affects the mixing length and eddy viscosity in the boundary layer [46].

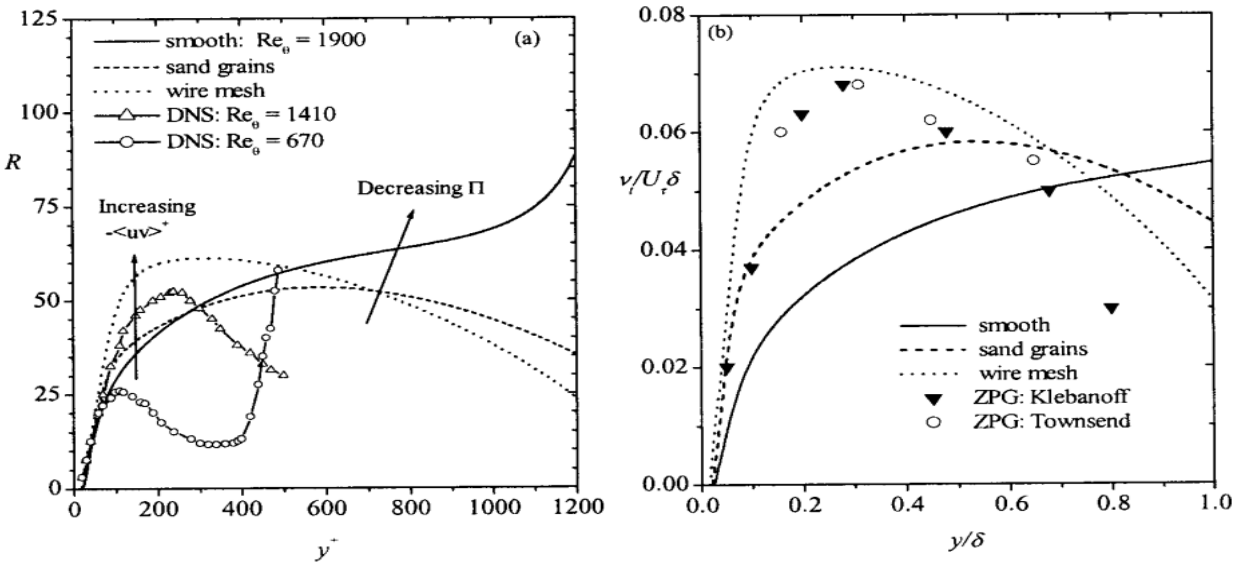

Figures 2.9a, 2.9b [46], depict the distribution of eddy viscosity and mixing length on both smooth and rough surfaces [47]. These figures can be incorporated into the discussion of how surface roughness alters the mixing length and eddy viscosity profiles, especially in the inner and outer regions of the boundary layer.

2.3.2.4. Conclusion

In conclusion, the study by Tachie, Bergstrom, and Balachandar [46] demonstrates that surface roughness significantly influences various turbulence statistics in an open channel flow. Surface geometry, and Reynolds number effects all play a crucial role in understanding the impact of roughness on turbulent boundary layers.

2.3.3 The work by Hayder Q Majeedl, Ali M.Ghazal and Basheer Al-Hadeethi [3 octobre 2022]

2.3.3.1 Aims of the Study

In this research by Hayder Q. Majeed, Ali M. Ghazal, and Basheer Al-Hadeethi [48], the goal was to explore how different shapes placed at the bottom of a water channel influence the characteristics of flowing water.

2.3.3.2 Experimental Setup and Procedure

The researchers [48] used a specialized laboratory for their experiments. Picture a long tank with clear walls and a steel floor that mimics a real river. They also had a way to control the water level. In this setup, they introduced two types of shapes on the channel's bottom: cubes and T-sections.

Figure 2.10: illustrates the experimental arrangement [48].

2.3.3.3 Results

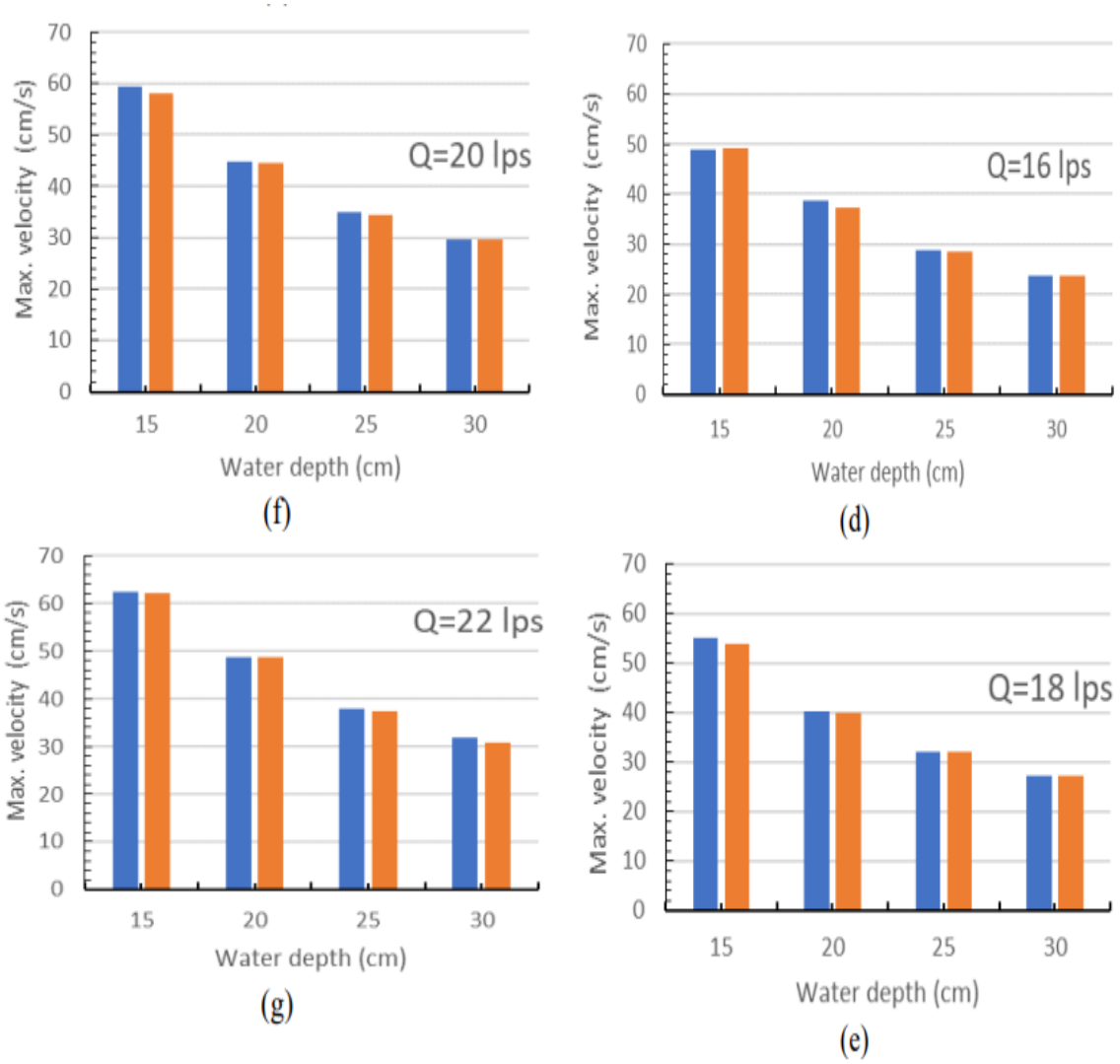

Figure 2.11: compares the water velocity in one section of the channel with cube-shaped roughness versus T-shaped roughness for different water flow rates [48]. It offers a comparative view of the two shapes' effects on flow.

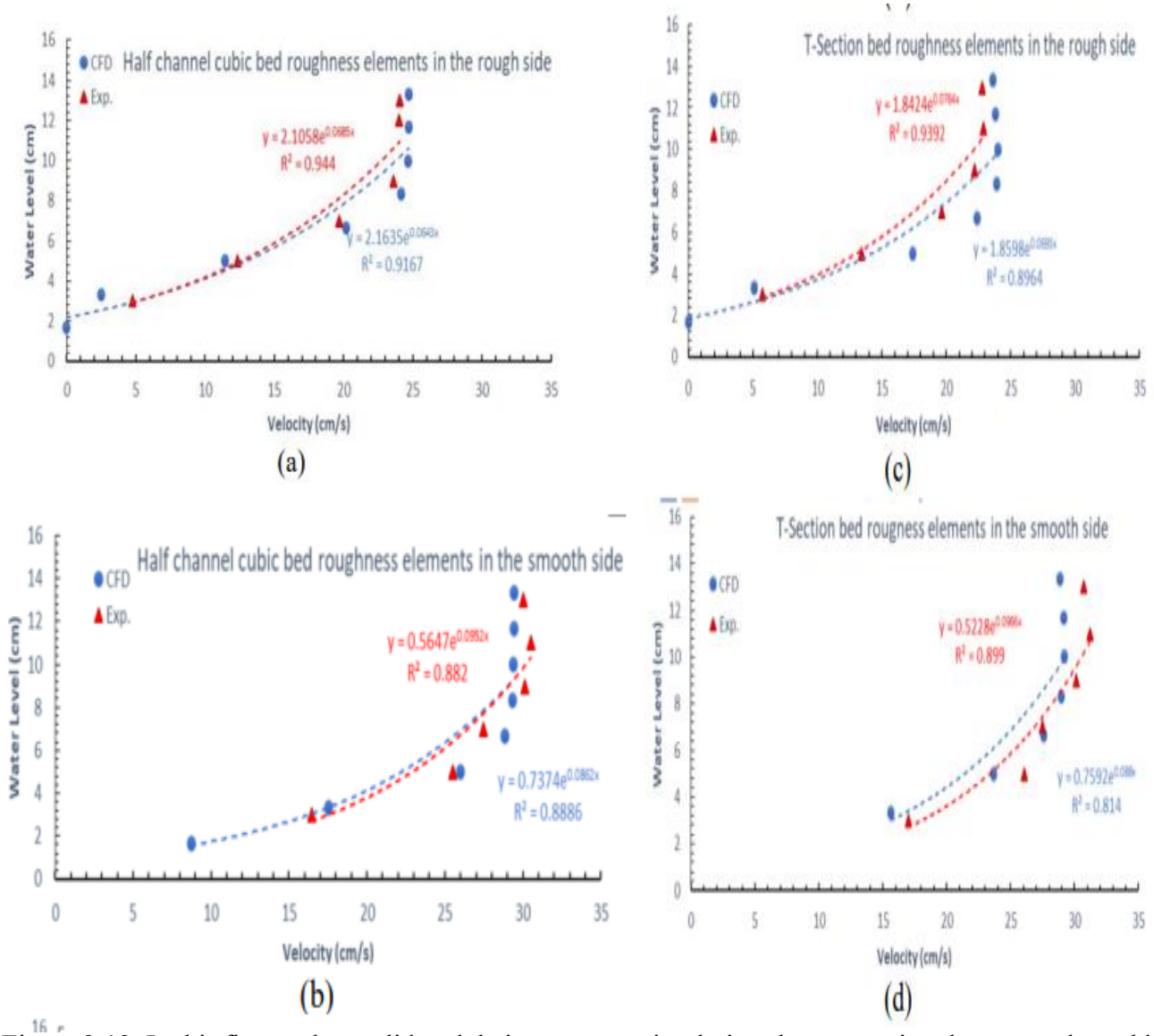

Figure 2.12: In this figure, they validated their computer simulations by comparing them to real-world experiments. It demonstrates the consistency between their computer models and actual experiments [48].

2.3.3.4 Discussion

This research by Hayder Q. Majeed, Ali M. Ghazal, and Basheer Al-Hadeethi [48] revealed several key findings:

Shape Matters: The choice of roughness shape significantly impacts the velocity profiles in an open channel. T-section bed roughness exhibited a noticeable influence on flow characteristics compared to cubic shapes [48].

Flow Rate Effects: The velocity distribution in open channels is sensitive to variations in flow rates. As flow rates increased, the velocity profiles changed accordingly [48].

Water Depth Matters: Altering water depths also played a role in influencing the velocity profiles. Changes in water depth led to corresponding adjustments in velocity distribution [48].

2.4. Conclusion

In summary, this chapter has taken us on a journey through the historical and scientific landscape of roughness effects on open channel flows, from the foundational work of Prandtl and Nikuradse to modern experiments and simulations. We have explored how rough surfaces influence the behaviour of turbulent flows. This knowledge is vital for understanding and managing open channel flows in various practical applications. As we move forward, we carry with us a deeper understanding of the complex interaction between roughness and turbulent flows in open channels.

Chapter 3: Methodology

3.1 Introduction

Imagine a river or an open channel of water. It might look calm on the surface, but beneath that surface, a lot is happening. This is where our study begins. We're on a mission to understand something crucial: how does the roughness of the surface, like the rocks or obstacles on the riverbed, affect the way water flows freely on top of it? It might sound simple, but it has big implications.

3.1.1 Aim of the Study

This work aims to study how surface roughness changes the way water moves in open channels. More precisely, we are interested in the scenario of the existence of the dip phenomenon, which occurs when the maximum velocity is below the free surface.

3.1.2 Why It Matters

This research is significant for several reasons. Engineers rely on this knowledge to improve water systems like those managing rivers and canals. It's also crucial for environmental scientists who study how water behaves on various surfaces, helping protect ecosystems by preventing erosion and preserving habitats. Overall, this research contributes to our understanding of how the natural world functions.

3.1.3 What's Ahead

In this chapter, we'll walk you through how we collected and prepared the data, and what we discovered about the fascinating relationship between surface roughness and free surface flows.

3.2 Gathering Data from Articles

We selected the article authored by Mark F. Tachie, Donald J. Bergstrom, and Ram Balachandar (2004) [46] as a cornerstone of our research. This article stood out because it offered crucial experimental data, including helpful figures, and provided in-depth information about test conditions and boundary layer parameters. It cantered on the complex relationship between surface roughness and turbulent boundary layers, specifically delving into the intriguing "dip phenomenon" and its impact on flow behaviour. These qualities made it a perfect match for our research goals, guiding our investigation effectively.

3.3 Data Extraction with Precision

To extract the vital data needed for our analysis, we employed a versatile tool known as the "Plot Digitizer"[51]. This software facilitated the precise extraction of information, including velocity profiles, surface roughness details, and other critical parameters that form the backbone of our comparative study.

3.4 A Study Without Experiments

Our research methodology was distinctive in not involving any physical experiments. Instead, our focus centred on the meticulous analysis of pre-existing data sourced from articles and other relevant literature. We chose this non-experimental approach primarily due to resource constraints. Unfortunately, our university lacks a laboratory facility, making it impossible for us to conduct experiments. Therefore, we relied on existing data from articles to pursue our research goals.

3.5 Unlocking Insights Through Velocity Profiles

Velocity profiles are crucial for our study because they serve as the foundation for our comparative analysis. We aim to compare computational velocity profiles generated through mathematical equations to pre-measured existing experimental data. By doing so, we can assess the accuracy of these equations in representing real-world scenarios. This comparison allows us to gain insights into how surface roughness affects water flow in open channels, a fundamental aspect of our research objectives.

Velocity profiles serve as the cornerstone of our study, offering a window into how water behaves in the presence of varying surface roughness conditions. These profiles were generated using MATLAB, a versatile computational tool, and analytical models derived from the research of Rafik Absi [52].

3.6 Equations for Velocity Profiles

We harnessed the power of mathematical equations to unveil the secrets hidden within these flows.In our situation where the dip phenomenon manifested, we turned to equations extracted from Rafik Absi's 2011 work [52]",

- **Differential Equation Describing Velocity Distribution and the Dip Phenomenon (Rafik Absi, 2011)**

In 2011, Rafik Absi [52] introduced the following ordinary equation to address the dip phenomenon observed in open channel flow:

$$\frac{dU_a}{d\xi} = \frac{1}{K}\left(1 - \alpha\frac{\xi}{1-\xi}\right)\left[\frac{1}{\xi} + \pi\Pi\sin(\pi\xi)\right] \quad (3.1)$$

When α equals 0 and Π takes values of 0.10 and 0.30 (Π is Coles parameter expressing the strength of the wake function). Equation (3.1) serves to determine the dip distance, denoted as ξ_{dip}, or the dimensionless distance from the bed corresponding to the maximum velocity, $U_{a,max} = U_a(\xi = \xi_{dip})$. Given that $dU_a/d\xi$ equals 0 at $\xi = \xi_{dip}$, the value of α can be calculated from Equation (3.2) as:

$$\alpha = \frac{1}{\xi_{dip}} - 1 \quad (3.2)$$

- **Simple dip-modified-log-wake law**

The "Simple Dip-Modified-Log-Wake Law" (sDMLW-law) is an equation used to model the velocity profiles in open-channel flows, particularly in cases where the conventional log-law doesn't match experimental data in the outer region (ξ>0.2). This equation is particularly useful when dealing with complex flows, like those with secondary currents in 3D channels [3].

$$U_a = \frac{1}{K}\ln\left(\frac{\xi}{\xi_0}\right) + \frac{2\Pi}{K}\sin^2\left(\frac{\pi}{2}\xi\right) + \frac{\alpha}{K}\ln(1-\xi) \quad (3.3)$$

It's important to note that these equations are typically applied to smooth surfaces, however, it's important to note that in our study, we weren't dealing with laboratory-smooth surfaces. Instead, with the complexities of roughness. To account for this, we introduced some modifications, known as the roughness function ΔU^+ to imitate the influence of surface roughness. This adaptation allowed us to capture the intricate dance of water flow over rough surfaces more accurately.

3.7 Solving the Equations

To solve these intricate equations, we didn't resort to manual calculations. Instead, we utilized the computational prowess of the "ode45" solver within MATLAB. This powerful tool efficiently and accurately solved the ordinary differential equation (ODE), enabling us to produce velocity profiles that faithfully mirrored the flow dynamics under diverse surface roughness scenarios.

Chapter 4: Data Analysis

4.1 Introduction

Welcome to the heart of our research. In this chapter, we dive into the data we've gathered from our sources and analyse it meticulously. We'll compare our findings with previous experiments, dissect the equations we've used, and, if applicable. This chapter is where we extract valuable insights and answers from the raw information, shedding light on the behaviour of water flow over rough surfaces.

4.2 Presentation of Velocity Profile Data

We extracted the measured data from an article by MF Tachie, DJ Bergstrom, and R Balachandar (2004) [46].

- **Experimental Setup and Procedure:**

The experiments were performed in an open channel flume that was 10 m long, 0.8 m wide, and 0.6 m deep. The sidewalls of the flume were made of tempered glass to facilitate optical access and flow visualization. The authors [46] measured the mean and fluctuating components of the streamwise velocity over smooth and three geometrically different types of surface roughness (sand grains, wire mesh, and perforated plate) using a laser Doppler anemometer. The study also measured the Reynolds stresses, turbulence kinetic energy, turbulence production and diffusion, and the distributions of eddy viscosity and mixing length in an open channel flow.

To understand the effects of roughness on open channel flows. We primarily extracted data from Table 4.1 [46], which provides essential test conditions and boundary layer parameters. The two key parameters of interest were the **smooth wall and sand grains.**

Test	U_e (cm/s)	δ (mm)	θ (mm)	Re_θ	U_τ (cm/s)	ΔU^+	π	Re_k	k_s^+
Smooth	49.2	38	3.87	1900	2.23		0.10		
Sand grains	53.1	37	4.11	2180	2.73	4.0	0.30	33	20
Wire mesh	53.4	38	4.91	2600	2.90	6.5	0.52	17	44

Table 4.1: Test conditions and boundary layer parameters [46]

In addition, we obtained experimental data by digitizing Figure 4.1 [46], with a specific focus on smooth and sand grain data. Figure 4.1 [46] illustrates the comparisons between computed velocity profiles and experimental data (symbols). Our examination of it unveiled the presence of the dip phenomenon, which is characterized by a maximum velocity occurring beneath the free surface.

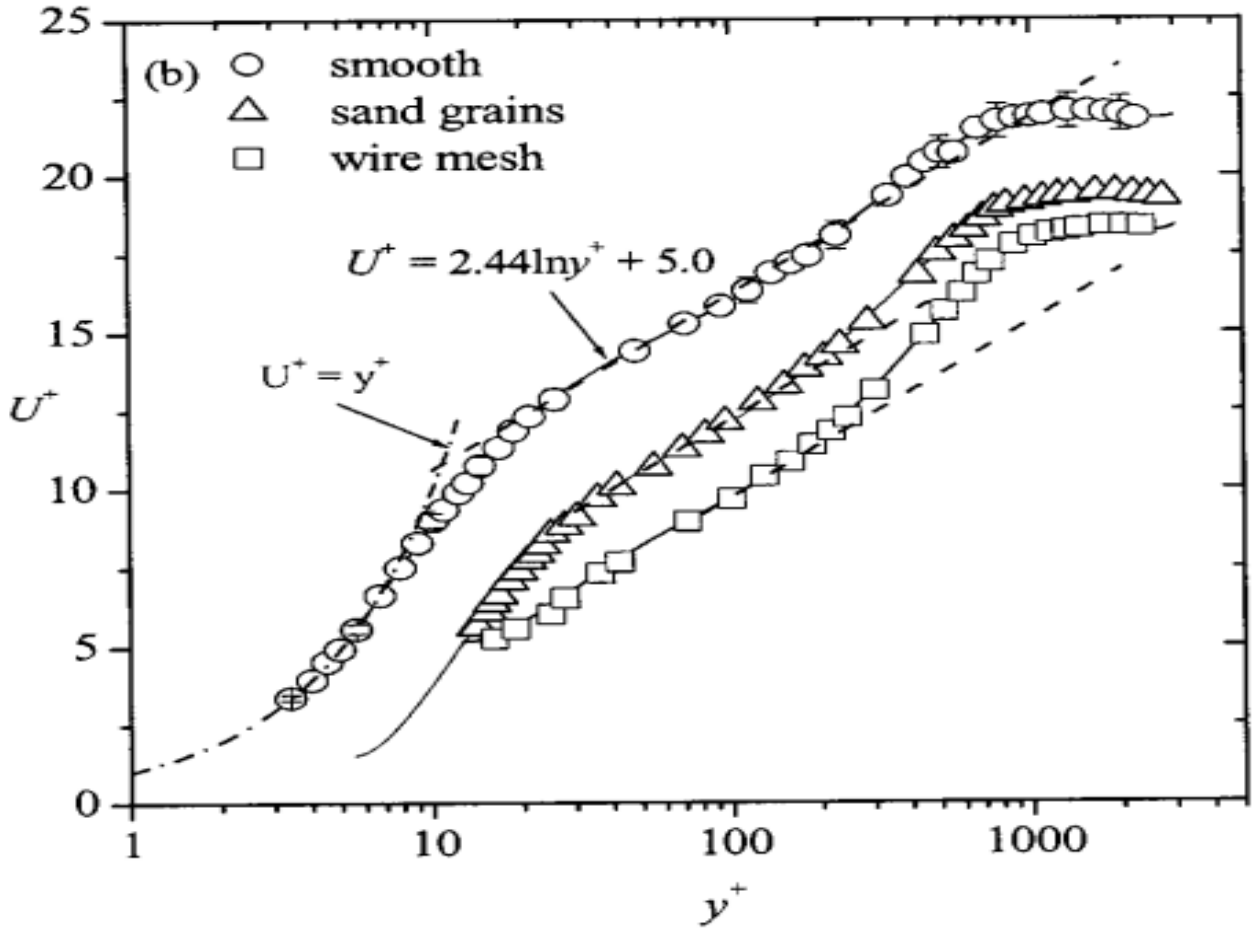

Figure 4.1: comparisons between computed velocity profiles and experimental data (symbols)[46].

To complement our analysis, "We have calculated the Reynolds friction number (Re_*) using the experimental data from Table 4.1 [46]. This parameter provides essential insights into the flow characteristics. The flow depth was 0.12 m, according to the information provided in [46], which states, 'The flow depth was maintained at h = 120 mm for all experiments. Additionally, we assumed a kinematic viscosity of 10^{-6} m²/s.

The equation used for calculating the Reynolds friction number is:

$$\mathbf{Re}_* = \frac{\mathbf{h}\,\mathbf{u}_*}{\boldsymbol{\nu}} \qquad (\mathbf{4.1})$$

Where:

- h represents the flow depth,
- u_* is the friction velocity ,
- ν denotes the kinematic viscosity.

Test	u_* (m/s)	h (m)	Re_*
Smooth	0,0223	0,12	2676
Sand grains	0,0273	0,12	3276

Table 4.2 : computed Reynolds friction number (Re_*)

The computed Reynolds friction number (Re_*) is vital in our MATLAB code because it defines flow conditions, sets initial conditions for solving equations, aids in comparing experimental and simulated profiles, and ensures dimensionless plotting, all crucial for understanding fluid flow over different surfaces.

4.3 Results and discussion :

Velocity profiles were generated for different values of Π (ranging from 0.10 to 0.30) [46] and α, which were determined based on estimated dip positions using Equation (3.2) . These profiles were then compared using the simple dip-modified-log-wake law (sDMLW-law, Equation) (3.3), numerical solutions of the ordinary differential equation (ODE) given by Equation(3.1), and experimental data from Tachie's study [46].

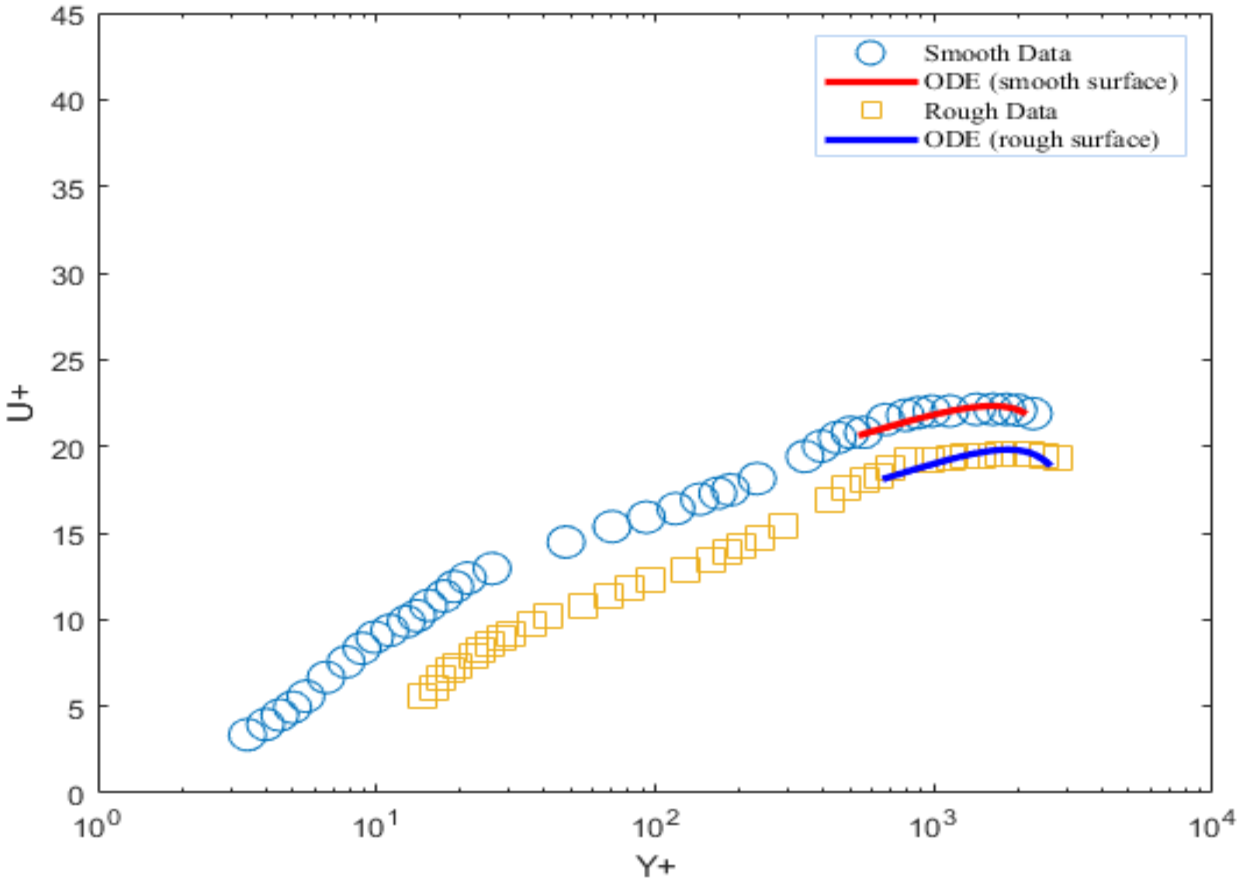

Figure 4.2: Velocity profiles obtained from (3.1) (blue and red solid lines); symbols: experimental data [46].

This figure displays predicted velocity profiles (U^+ (Y^+)) and offers a comparison between velocity profiles obtained from Equation (3.1) sourced from the article [52] – and experimental data gathered by Mark F. Tachie in 2004 [46].

4.3.1 Figures 4.2 analysis:

- **Consistency and Agreement:** The figure reveals a striking similarity between the calculated velocity profiles and the experimental data. This means that the equation we used to model the flow, called the Ordinary Differential Equations (ODE) model, seem to be doing a good job replicating what happens in real-world open channel flows.
- **Rough vs. Smooth Surfaces:** It's crucial to notice that the velocity profiles are different for rough and smooth surfaces. For rough surfaces, there's a noticeable drop in the velocity compared to smooth surfaces characterized by a downward shift emulated by a roughness function ($\Delta U^+ = 3$).

This suggests that roughness elements on the bed have a significant impact on how the flow behaves close to the surface.

- **The Dip Phenomenon:** The ODE model also captures something known as the "dip phenomenon." This means that there's a specific point, represented by ξ_{dip}, where the velocity reaches its maximum value, and it's a bit away from the bed. This dip phenomenon is a key characteristic of turbulent open channel flows.
- **Validity of the ODE Model:** The fact that our calculated profiles match the experimental data suggests that the ODE model, based on the work of Rafik Absi, is a valid way to describe how velocity varies on open channel flows. However, it's important to recognize that this model has its own set of mathematical assumptions and limitations.

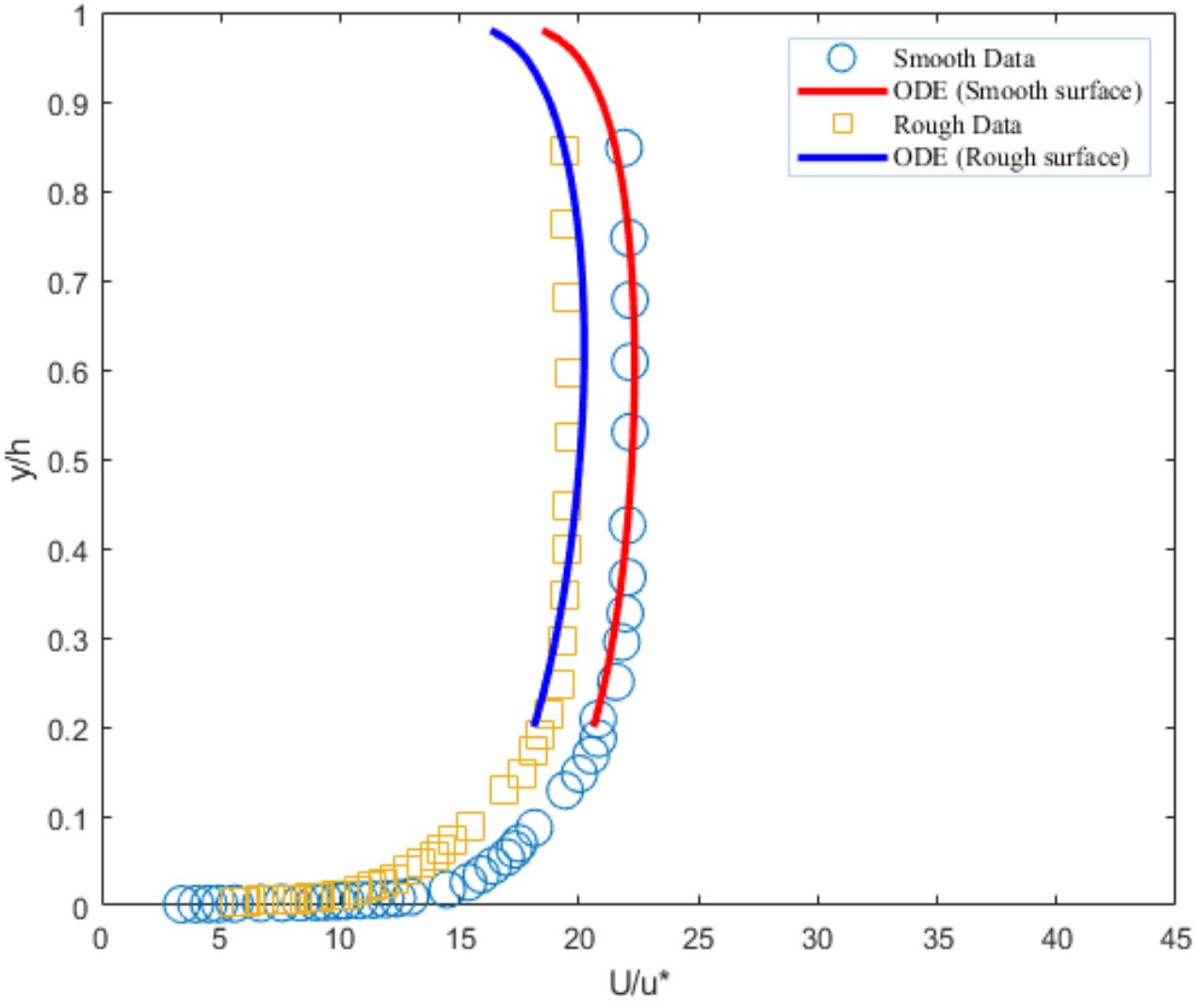

Figure 4.3: Velocity profiles obtained from (3.1) (blue and red solid lines); symbols: experimental data (symbols) [46].

This figure showcases a comparison of velocity profiles (y/h (U^+)) obtained from Equation (3.1). This includes $\Pi = 0.10$ for the smooth surface and $\Pi = 0.30$ for the rough surface. We also adjusted α values based on estimated dip positions (3.2) and calibrated them further to achieve better alignment with the measured data [56]. A boundary condition was applied at $\xi = 0.2$.

4.3.2 Figure 4.3 Analysis:

- **Alignment with Experimental Data:** The computed velocity profiles match well with the experimental data. We intentionally used a roughness function with a value of ($\Delta U+ = 3$) to emulate the effect of the velocity shift caused by surface roughness as a leftward shift, to make it align with the rough experimental data.
- **Calibration for Accuracy:** We Adjusted the model by introducing a roughness function ($\Delta U^+ = 3$) to ensure that the model accurately mimics the behaviour seen in rough surface conditions. This demonstrates the model's adaptability.
- **Alignment in the Outer Region (y/h > 0.2):** The computed profiles and experimental data align well at $y/h > 0.2$. This confirms that the model accurately captures how the flow behaves, especially away from the bed, which is vital for practical applications.

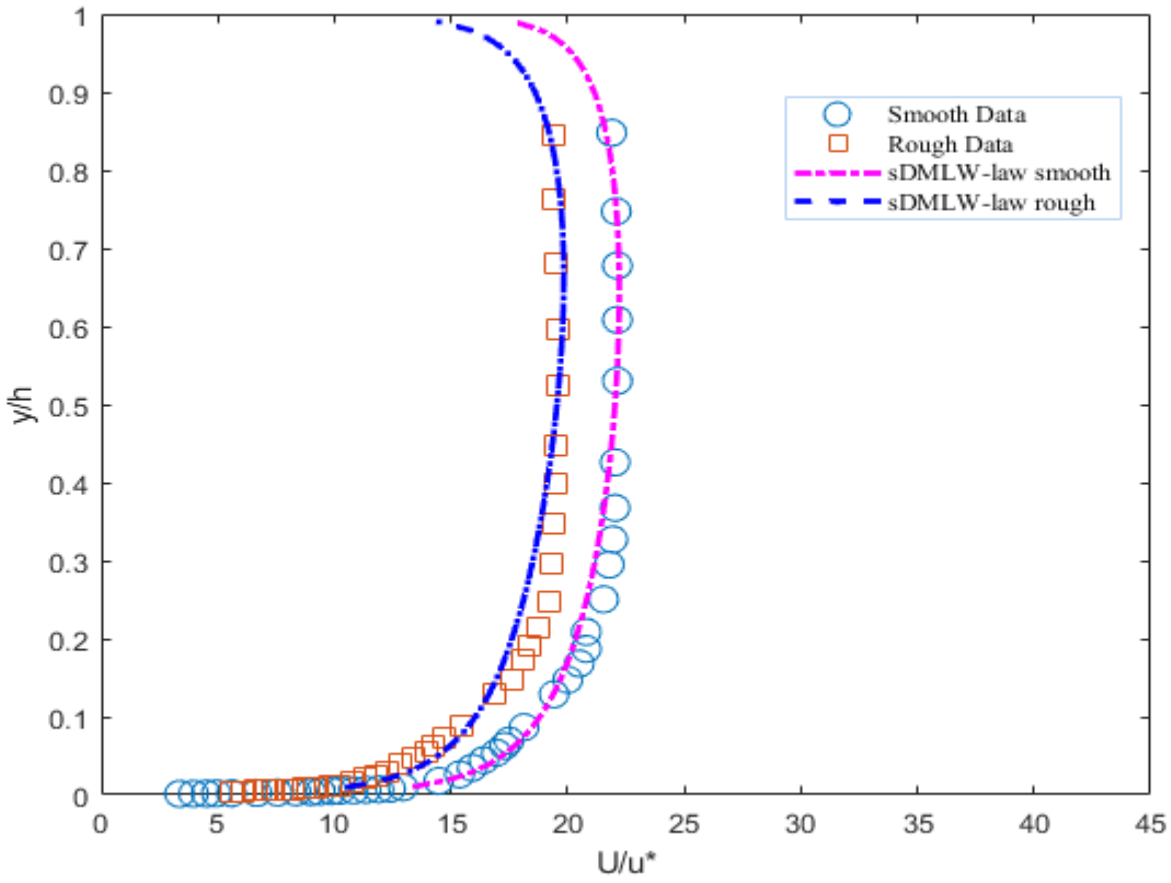

Figure 4.4: Velocity profiles obtained from (3.3) (blue and magenta dashed lines); equation (3.3), symbols: experimental data(symbols) [46].

This figure offers a comparison of computed velocity profiles derived from sDMLW-law (3.3) – and experimental data by Mark F. Tachie in 2004 [46].

4.3.3 Figure 4.4 Analysis:

Our analysis of this figure indicates a concordance between the computed velocity sDMLW-law (3.3) profiles and the corresponding experimental data [46], particularly in the outer region ($\xi > 0.2$). Remarkably, in the case of rough surfaces, we notice a shift in the computed profile sDMLW-law (3.3) that closely mirrors the behaviour observed in the measured rough data.

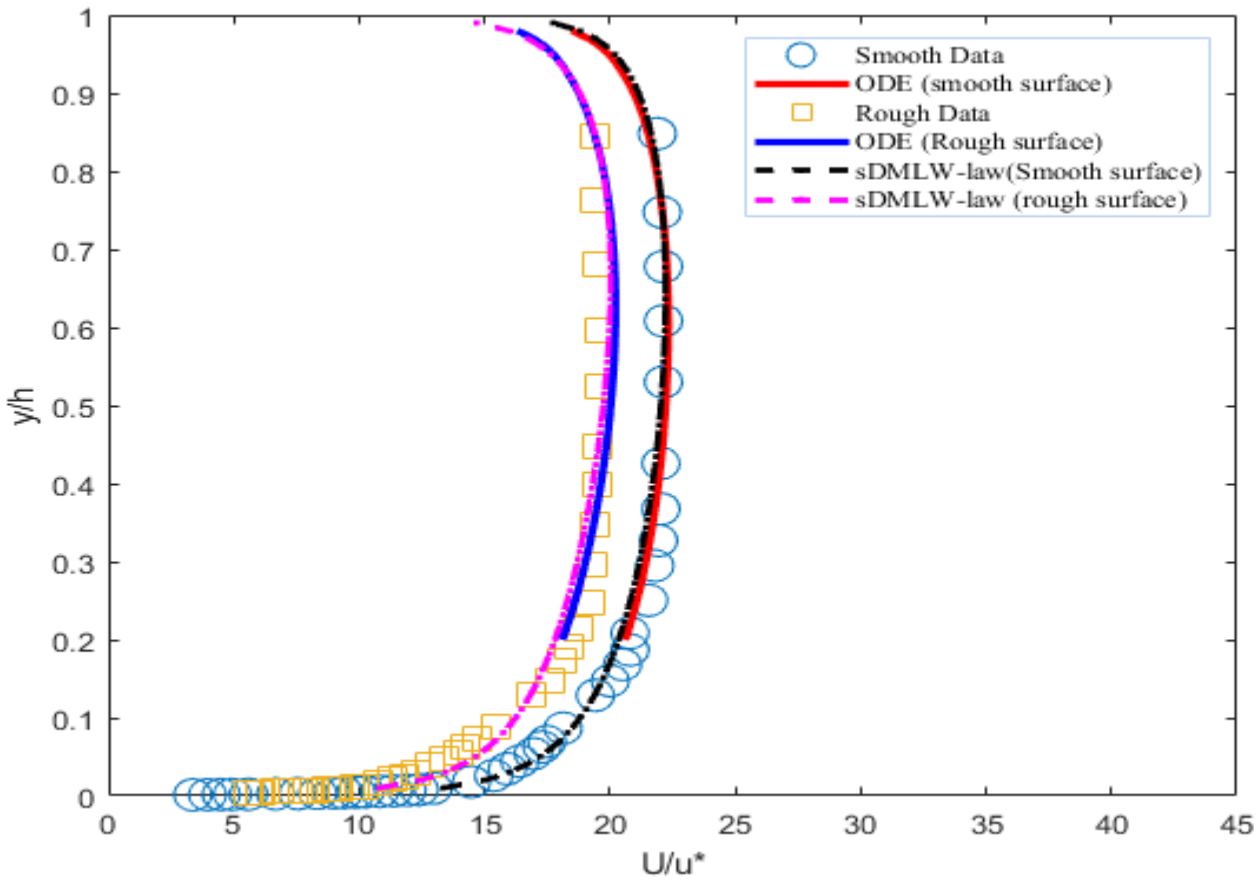

Figure 4.5: presents a comparison between computed velocity profiles using Equation (3.1) (red and blue solid lines) and Equation (3.3) (magenta and black dashed lines), along with measured data from Tachie in 2004 (symbols) [46].

4.3.4 Figure 4.5 Analysis:

The profiles derived from the Ordinary Differential Equation (ODE) Equation (3.1) and the Simple Dip-Modified-Log-Wake Law (sDMLW-law) Equation (3.3) exhibit a strong alignment and close correspondence, particularly in the outer region ($\xi > 0.2$).

Both the ODE and sDMLW-law profiles demonstrate a match with the measured data [46], especially in the outer region, regardless of whether the surface is smooth or rough.

In the case of rough surfaces, we discern a shift in the computed profiles that closely replicates the behaviour observed in the measured rough data.

4.4 Summarization of the key findings

4.4.1 Our research has uncovered vital insights:

- **Roughness Effect:** roughness on the surface has an important role in altering the behaviour of flowing water. It is especially remarkable when we observe rough profiles.
- **Profile Shift:** When dealing with rough surfaces, we consistently observed a distinctive shift in both computational (3.1) (3.2) and experimental velocity profiles [46]. This shift is a critical indicator of how surface roughness influences flow dynamics. We can hypothesize that this shift is caused by a drop in velocity for rough surfaces because of the interaction between the flowing water and the roughness elements on the bed. These elements disrupt the flow, creating more turbulence and changing how fast the water moves at different heights above the bed.
- **Roughness function:** To accurately model profiles using the ordinary Differential Equation (3.1), we had to incorporate a wall function (ΔU^{+}). This adjustment allowed us to closely replicate the observed shift in the measured data.
- **Simple dip-modified-log-wake law:** The application of the Simple Dip-Modified-Log-Wake Law (3.3) to generate velocity profiles resulted in close agreement with experimental data [46], especially in the outer region $\xi > 0.2$.
- **Alignment with Experimental Data and Matching Computer Models with Reality :** Our research findings reveal a remarkable convergence between computational velocity profiles (3.1) (3.3) and pre-existing experimental data [46]. This harmony signifies that the computational models employed have succeeded in accurately replicating and predicting how water behaves over rough surfaces.
- **Why This Matters:** Our research is important because it confirms that these computer models are accurate, especially when dealing with complex flows and rough surfaces. This is like having a reliable compass that helps engineers and environmental scientists navigate the complex world of fluid dynamics, even in challenging conditions.
- **Limitations and Accuracy:** We need to remember that our findings are based on the quality of the original data we used. If the data is off, it's like using a map with mistakes.
- **Practical Benefits:** The practical side of our work is like giving engineers and environmental scientists a super tool. These validated computer models can help them design water systems that work well, protect against things like erosion, and keep our natural world safe. It's like handing them a treasure map to safeguard our environment.

General Conclusion

In this study, we embarked on a mission to investigate the complex relationship between surface roughness and water flow in open channels. Our primary research objectives were to understand how the presence of roughness elements on the bed influences the velocity distribution particularly on the presence of the "dip phenomenon", validate computational models, and examine the practical applications of our findings. We recognized the importance of this research in improving water systems, safeguarding ecosystems, and advancing our understanding of fluid dynamics.

Our research uncovered several key findings and insights:

Roughness Effect: We observed that surface roughness plays a pivotal role in altering the behaviour of flowing water. Specifically, rough surfaces exhibited distinctive effects on velocity profiles, with a noticeable shift caused by the presence of roughness elements on the bed. This disruption led to increased turbulence and variations in flow velocity at different heights above the bed.

Profile Shift: Across both computational and experimental data, we consistently observed a significant shift in velocity profiles for rough surfaces compared to smooth surfaces. This shift, indicative of surface roughness influence, was accurately captured by introducing a wall function ($\Delta U+$) in the computational models.

Validation of Models: Our findings confirmed the effectiveness of the Ordinary Differential Equation (ODE) model and the Simple Dip-Modified-Log-Wake Law (sDMLW-law) based on Rafik Absi's work (2011) in replicating and predicting real-world open channel flow behaviors.

Implications for Engineering and Environmental Science

Engineering Benefits: The validated computational models can be a game-changer for engineers working on water systems. They provide a reliable framework for designing systems that can mitigate challenges like erosion, optimize water flow, and ensure the efficient management of water resources.

Environmental Protection: By better understanding how water behaves on various surfaces, our research contributes to the protection of ecosystems. It empowers environmental scientists to develop strategies that safeguard habitats and prevent detrimental impacts, such as sediment erosion.

Limitations and Future Research

While our research has provided valuable insights, it is important to acknowledge its limitations. The accuracy of our findings is dependent on the quality of the original data used. Future research endeavours should focus on improving data collection and refining computational models for even more accurate predictions.

In conclusion, our study not only deepens our comprehension of fluid dynamics but also offers a practical compass for professionals in the fields of engineering and environmental science. We are excited about the potential benefits that this research can bring, such as improved water management, preservation of natural habitats, and the protection of our environment.

References

[1] Kármán, T. von. (1937). On the statistical theory of turbulence. Proceedings of the National Academy of Sciences of the United States of America, 23(2), 98-105.

[2] da Vinci, L. (1452-1519). Observations on the formation of vortices and their interactions. [Manuscript]. Biblioteca Ambrosiana, Milan, Italy.

[3] Absi, R. (2021). Reinvestigating the parabolic-shaped eddy viscosity profile for free surface flows. Hydrology, 8(3), 126.

[4] Pope, S. B. (2000). Turbulence modeling. Cambridge University Press, New York.

[5] Reynolds, O. (1883). An experimental investigation of the circumstances which determine whether the motion of water shall be direct or sinuous, and of the law of resistance in parallel channels. Philosophical Transactions of the Royal Society of London, 174, 935-982.

[6] Prandtl, L. (1904). Über Flüssigkeitsbewegung bei sehr kleiner Reibung. Proceedings of the Third International Congress of Mathematicians, Heidelberg, 484-491.

[7] Nikuradse, J. (1933). Gesetzmäßigkeiten der turbulenten Strömung in glatten Rohren (Nachtrag). Forschung auf dem Gebiet des Ingenieurwesens A, 4(1), 44-44.

[8] J. Jimenez. (2004), Turbulent lows over rough walls, Annu. Rev. Fluid Mech. 36 (2004)173–196,

[9] Cebeci, T. (2004). Turbulence Models and Their Application: Efficient Numerical Methods with Computer Programs. Springer Science & Business Media.

[10] Cheng, H., & Castro, I. P. (2002). Near-wall flow over urban-like roughness. Boundary-Layer Meteorology, 104(2), 229-259.

[11] Hama, F. R. (1954). Boundary layer characteristics for smooth and rough surfaces. Transactions of the Society of Naval Architects and Marine Engineers, 62, 333–358.

[12] Nezu, I., Tominaga, A., & Nakagawa, H. (1993). Field measurements of secondary currents in straight rivers. Journal of Hydraulic Engineering, 119(5), 598-614.

[13] Nezu, I., & Nakagawa, H. (1984). Cellular secondary currents in straight conduit. Journal of hydraulic engineering, 110(2), 173-193.

[14] Nezu, I., & Rodi, W. (1985). Secondary currents in turbulent channel flows. Journal of Fluid Mechanics, 157, 289-319.

[15] Nezu, I., & Nakagawa, H. (1984). Secondary currents in turbulent channel flows with heterogeneous roughness. Journal of Fluid Mechanics, 140, 221-252.

[16] Wang, Y., Wang, X., & Zhang, L. (2001). Dip phenomenon in turbulent open channel flows with heterogeneous roughness. Journal of Hydraulic Engineering, 127(12), 1145-1154

[17] Jaywant H. Arakeri and P. N. Shankar, (2000), Ludwig Prandtl and boundary layers in fluid flow, Resonance, the Indian Academy of Sciences, vol:5, pages:48-63.

[18] Prandtl, L. (November 1940). Note On The Calculation Of Boundary Layers. National Advisory Committee for Aeronautics, vol 18,16 pages.

[19] Nikuradse, J. (1950). Laws Of Flow In Rough Pipes, National Advisory Committee For Aeronautics Technical Memorandum 1292.

[20] Chedevergne, F., & Aupoix, B. (2017, July). Accounting for wall roughness effects in turbulence models: a wall function approach. In 7th European conference for aerospace sciences (EUCASS), Milan, Italy (pp. 3-6).

[21] Grigson, C. (1987). The full-scale viscous drag of actual ship surfaces and the effect of quality of roughness on predicted power. Journal of ship research, 31(03), 189-206.

[22] Karman, T. (1930). von: Mechanische Ähnlichkeit und Turbulenz, Nachr. Ges. Wiss. Göttingen, Math.-phys. Kl.(1930) 58–76'. Proc. 3. Int. Cong. Appl. Mech, 322.

[23] Von Kármán, T. (1921). Uber laminare und turbulente Reibung. Z. Angew. Math. Mech., 1, 233-252.

[24] Schlichting, H. (1968). Boundary Layer Theory. Hcgraw-Hill Book Company. New York, N. Y, 586.

[25] Van Driest, E. R. (1956). On Turbulent Flow Near a Wall. Journal of the Aeronautical Sciences, 23(11), 1007-1011.

[26] Krogstad, P. A. (1991). Modification Of the Van Driest Damping Function To Include The Effects Of Surface Roughness. AIAA Journal, 29(6), 888-894.

[27] Kazemi, E., Nichols, A., Tait, S., & Shao, S. (2016). SPH Modelling Of Depth-Limited Turbulent Open Channel Flows Over Rough Boundaries. In Proceedings of the International Conference on Computational Fluid Dynamics (pp. 45-58). XYZ Publications.

[28] Kazemi, E. (2017). Numerical Modelling Of Turbulent Free Surface Flows Over Rough And Porous Beds Using The Smoothed Particle Hydrodynamics Method.

[29] Chedevergne, F., & Forooghi, P. (2020). On the importance of the drag coefficient modelling in the double averaged Navier-Stokes equations for prediction of the roughness effects. Journal of Turbulence, 21(8), 463-482.

[30] Chedevergne, F. (2021). A double-averaged Navier-Stokes k–ω turbulence model for wall flows over rough surfaces with heat transfer. Journal of Turbulence, 22(11), 713-734.

[31] Anderson, J. D., & Wendt, J. (1995). Computational fluid dynamics (Vol. 206, p. 332). New York: McGraw-hill.

[32] Zawawi, M. H., Saleha, A., Salwa, A., Hassan, N. H., Zahari, N. M., Ramli, M. Z., & Muda, Z. C. (2018, November). A review: Fundamentals of computational fluid dynamics (CFD). In AIP conference proceedings (Vol. 2030, No. 1). AIP Publishing.

[33] Kirkgöz, M. S. (1989). Turbulent velocity profiles for smooth and rough open channel flow. Journal of Hydraulic Engineering, 115(11), 1543-1561.

[34] Cebeci, T., & Smith, A. M. O. (1974). Analysis of turbulent boundary layers. NASA STI/Recon Technical Report A, 75, 46513.

[35] Klebanoff, P. S. (1954). Characteristics Of Turbulence In A Boundary Layer With Zero Pressure Gradient. NACA Technical Notes, No. 3178, Washington, D.C.

[36] Prandtl, L. (1925). Über Die Ausgebildete Turbulenz. Z. Angew. Math. Mech., Bd. 5, 136-139 (In German).

[37] Prandtl, L. (1932). Zur Turbulenten Stromung In Rohren Und Langs Platten. Ergebnisse Der Aerodynamischen Versuchsanstalt Zu Göttingen, 4, 18-29 (In German).

[38] Coles, D. (1956). The law of the wake in the turbulent boundary layer. Journal of Fluid Mechanics, 1(2), 191-226.

[39] Coles, D. (1955). The law of the wall in turbulent shear flow. 50 Jahre Grenzschichtforschung: Eine Festschrift in Originalbeiträgen, 153-163.

[40] Mikhailov, V. V. (2005). Universal velocity defect law for the turbulent boundary layer. Fluid Dynamics, 40(2), 245-255.

[41] Bayazit, M. (1976). Free Surface Flow In A Channel Of Large Relative Roughness. Journal of Hydraulic Research, 14(2), 115-126.

[42] Kamphuis, J. W. (1974). Determination Of Sand Roughness For Fixed Beds. Journal of Hydraulic Research, 12(2), 193-203.

[43] Hinze, J. O. (1975). Turbulence McGraw-Hill. Publi, New York, USA.

[44] Zippe, H. J., & Graf, W. H. (1983). Turbulent Boundary-Layer Flow Over Permeable And Non-Permeable Rough Surfaces. Journal of Hydraulic Research, 21(1), 51.

[45] Rotta, J. C. J. (1962). Turbulent boundary layers in incompressible flow. Progress in aerospace sciences, 2(1), 1-95

[46] Tachie, M. F., Bergstrom, D. J., & Balachandar, R. (2004). Roughness effects on the mixing properties in open channel turbulent boundary layers. J. Fluids Eng., 126(6), 1025-1032.

[47] Tachie, M. F., Bergstrom, D. J., & Balachandar, R. (2002). The Effect of Wall Roughness on an Open Channel Boundary Layer. In Engineering Turbulence Modelling and Experiments 5 (pp. 455-463). Elsevier Science Ltd.

[48] Majeed, H. Q., Ghazal, A. M., & Al-Hadeethi, B. (2022). Experimental and Numerical Study of Open Channel Flow with T-Section Artificial Bed Roughness. Mathematical Modelling of Engineering Problems, 9(6).

[49] Clauser, F. H. (1956). The turbulent boundary layer. Advances in applied mechanics, 4, 1-51.

[50] Clauser, F. H. (1954). Turbulent boundary layers in adverse pressure gradients. Journal of the Aeronautical Sciences, 21(2), 91-108.

[51] Rohatgi, A. (2020). WebPlotDigitizer user manual.

URL: https://automeris. io/WebPlotDigitizer/userManual. pdf (05.08. 2021.).

[52] Absi, R. (2011). An Ordinary Differential Equation For Velocity Distribution And Dip-Phenomenon In Open Channel Flows. Journal Of Hydraulic Research, 49(1), 82-89.

[53] Sill, B. L. (1982). New Flat Plate Turbulent Velocity Profiles. Journal of Hydr. Engineering, ASCE, 108(1), 1-15.